Air particulate matter composition, sources and trends in the Whangarei Airshed

P. K. Davy T. Ancelet

GNS Science Consultancy Report 2014/186
December 2014 FINAL

GNS SCIENCE
TE PŪ AO

DISCLAIMER

This report has been prepared by the Institute of Geological and Nuclear Sciences Limited (GNS Science) exclusively for and under contract to Northland Regional Council. Unless otherwise agreed in writing by GNS Science, GNS Science accepts no responsibility for any use of or reliance on any contents of this Report by any person other than Northland Regional Council and shall not be liable to any person other than Northland regional Council, on any ground, for any loss, damage or expense arising from such use or reliance.

The data presented in this Report are available to GNS Science for other use from August 2014.

BIBLIOGRAPHIC REFERENCE

Davy, P. K.; Ancelet, T. 2014. Air particulate matter composition, sources and trends in the Whangarei Airshed, *GNS Science Consultancy Report* 2014/186. 58 p.

CONTENTS

FIGURES

TABLES

APPENDICES

APPENDIX FIGURES

EXECUTIVE SUMMARY

This report presents an analysis of 7 years (2004–2012) of air particulate matter (PM_{10}) samples from Whangarei. This work was commissioned by the Northland Regional Council (NRC) to data-mine the sample set in order to understand the sources contributing to ambient particulate matter concentrations. The study was partially funded by an Envirolink grant from the Ministry of Business, Innovation and Employment.

The elemental composition of PM_{10} in each sample was determined and the data was used as the basis for identifying the sources contributing to PM_{10} in the Whangarei airshed. The temporal patterns and trends of the contributing sources were then used to explain the observed PM_{10} concentrations at the monitoring site.

Sources of PM_{10} in Whangarei

Four sources were extracted from the PM_{10} elemental composition data by receptor modelling techniques to identify the primary contributing sources to PM_{10} in the Whangarei airshed. The four sources were identified to be:

1. A combined motor vehicle and crustal matter source;
2. Marine aerosol (seasalt);
3. Biomass burning (wood fires for home heating);
4. Secondary sulphate.

Figure ES1 presents the relative contribution of the sources to PM_{10} concentrations. Similar source contribution profiles have been established for other towns and cities across New Zealand.

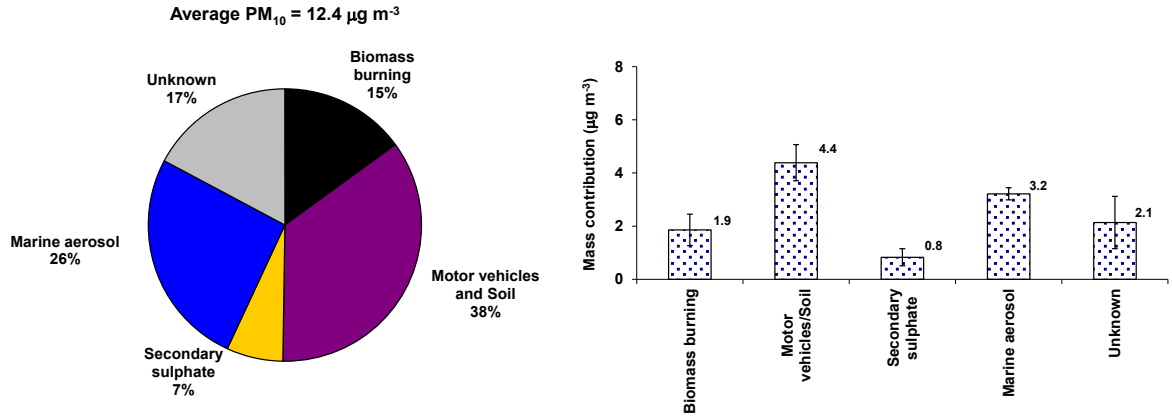

Figure ES1 Average (2004–2012) relative source contributions to PM_{10} at Water Street.

The source chemical profiles and the temporal variations in the PM_{10} source contributions were considered to be strongly representative of the identified sources. It was evident that PM_{10} mass was dominated by the biomass combustion source during winter, which arises primarily from solid fuel (wood burning) fire emissions used for domestic heating. During other time periods, motor vehicles, crustal matter and marine aerosol were the primary sources of particulate matter at the Water Street site.

PM_{10} Composition

Due to filter matrix effects, some elemental concentrations could not be determined or had analytical uncertainty that was propagated to the source contribution results and this uncertainty is likely to explain the 'Unknown' (or indeterminate) component identified in Figure ES1. It was found that BC was an important component of PM_{10} as an indicator of combustion source emissions. Chlorine and sulphur had the second and third highest average concentrations respectively. Arsenic and lead were found to be present in PM_{10} samples at concentrations above their limits of detection and the time series for both elements showed winter peaks in concentrations as shown in Figure ES2.

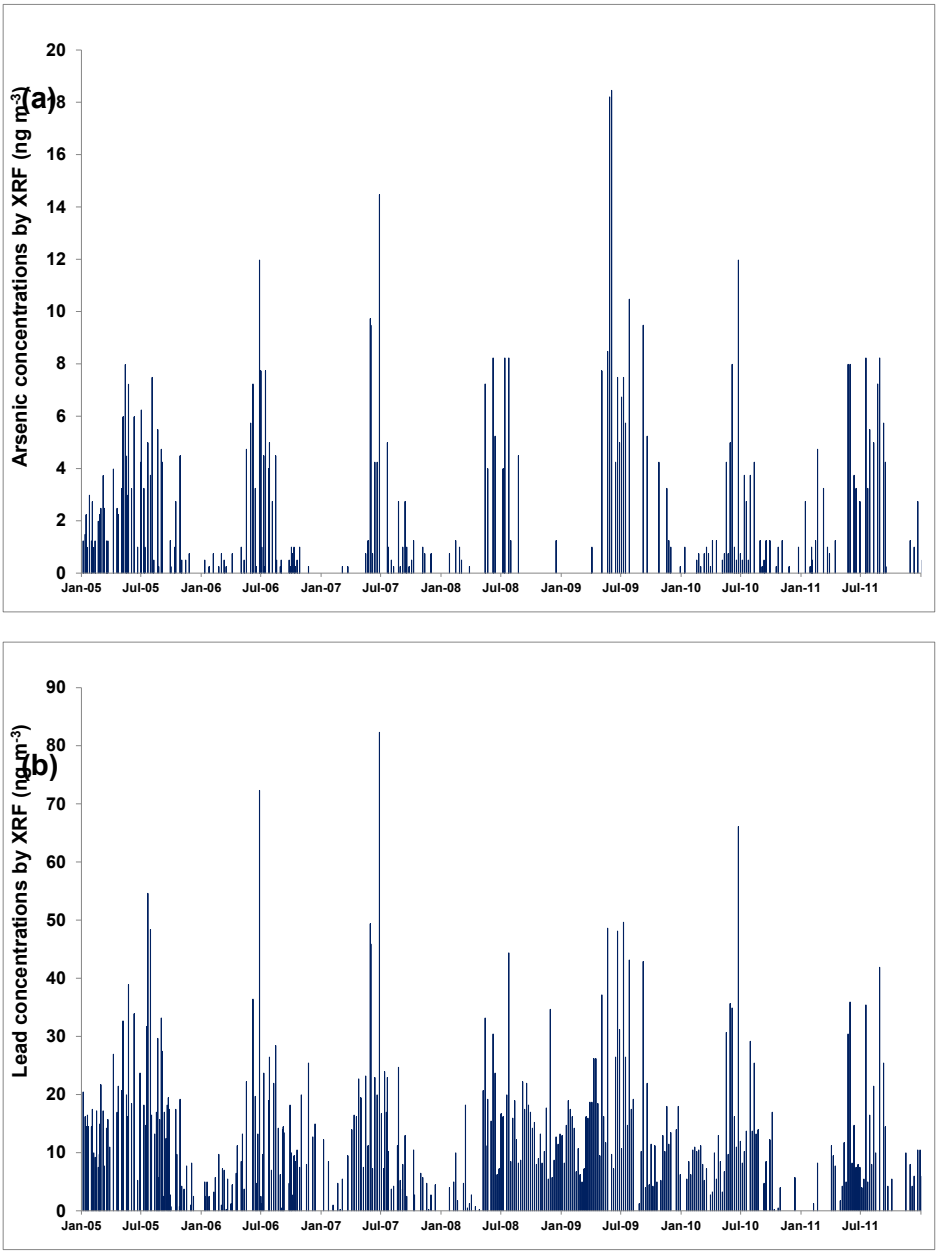

Figure ES2 (a) Arsenic concentrations and (b) Lead concentrations at the Water Street site.

Both arsenic and lead were strongly associated with the biomass combustion source and this was considered to be through the use of copper chrome arsenate treated timber and timber that had been painted with lead containing paints as fuel in domestic fires.

Trends in PM_{10} concentrations and source contributions

The data were examined for temporal trends and it was found that both PM_{10} and black carbon concentrations were decreasing over the 7-year monitoring period. When the black carbon data were broken down by combustion source contributions it was found that there was a decreasing trend in biomass burning (and by inference a reduction in domestic fire emissions) and that this was driving the reduction in PM_{10} concentrations. No significant trend was evident for the motor vehicle combustion source.

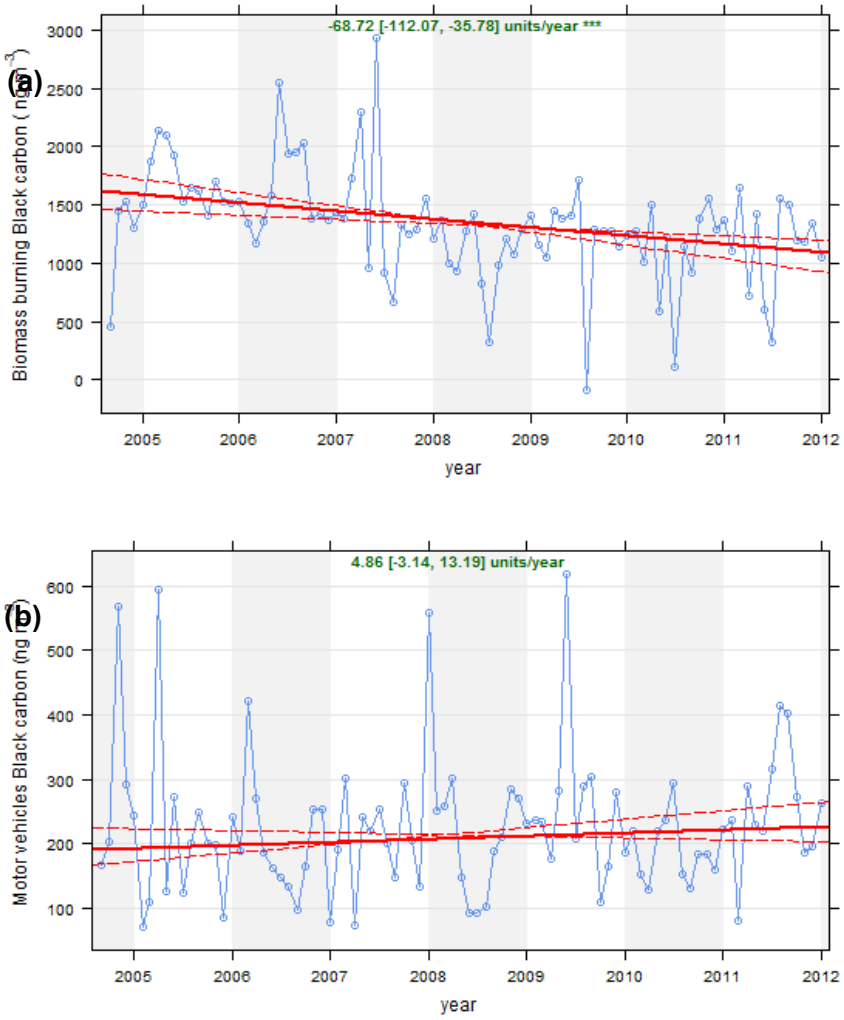

Figure ES3 Trend analysis (deseasonalised) for biomass combustion (a) and motor vehicle-related (b) black carbon concentrations at the Water Street site. The solid red lines indicate the trend estimates, while the dashed red lines indicate the 95% confidence intervals based on data resampling methods.

Overall the trending reduction in PM_{10} concentrations due to decreasing domestic fire emissions is a positive outcome for air quality management in the Whangarei airshed and the associated human health implications from exposure to this source. However, the presence of arsenic and lead in PM_{10} associated with domestic fire emissions raises questions as to why fuels contaminated with these elements are finding their way into the fuel supply. This is particularly relevant since use of such contaminated fuel is banned by the Regional Air Plan.

Moreover, the Water Street monitoring site was located in the CBD area of Whangarei City and was therefore somewhat removed from the residential locations where emissions were likely to occur. Consequently the measured elemental concentrations for species such as arsenic and lead at Water Street would be less than in a residential area and therefore the true exposure to these contaminants may be higher. Consideration should also be given to indoor air quality in the houses of those residents who use such contaminated fuels and the potential for adverse health effects on the inhabitants.

Recommendations

Given the presence of arsenic and lead contamination in PM_{10} and the link to domestic wood fires, Northland Regional Council may wish to consider monitoring campaigns to investigate the extent of the problem with a particular focus on residential locations where exposure is likely to be highest (i.e., neighbourhoods with a high percentage of domestic solid fuel fires).

1.0 INTRODUCTION

This report presents an analysis of 7 years of air particulate matter samples from the city of Whangarei, located in the north of New Zealand's North Island. This work was commissioned by the Northland Regional Council (NRC) to understand the sources contributing to ambient particulate matter concentrations and was partially funded by an Envirolink grant (1409-NLRC165) from the Ministry of Business, Innovation and Employment.

The particulate matter monitoring by the Northland Regional Council (NRC) was aimed at monitoring PM_{10} concentrations (particles which have an effective aerodynamic cross-section less than 10 μm). NRC used the gravimetric mass results to assess compliance with the New Zealand National Environmental Standard for Air Quality for PM_{10} (set at 50 μg m^{-3} 24-hour average).

1.1 REQUIREMENT TO MANAGE AIRBORNE PARTICLE POLLUTION

As a result of urban air pollution in towns and cities across New Zealand, particularly during the winter, and in response to growing evidence of significant health effects associated with airborne particle pollution, the New Zealand Government introduced a National Environmental Standard (NES) in 2005 of 50 μg m^{-3} for PM_{10}. The NES places an onus on regional councils to monitor PM_{10} and publicly report the results if the air quality in their region exceeds the standard. Initially, regional councils were required to comply with the standard by 2013 or face restrictions on the granting of resource consents for discharges that contain PM_{10}, but the NES has since been revised, extending the target date for regional councils to comply with the standard. The new target dates are September 1, 2016 for airsheds with between 1 and 10 exceedances and September 1, 2020 for airsheds with 10 or more exceedances. In areas where the PM_{10} standard is exceeded, information on the sources contributing to those air pollution episodes is required to effectively manage air quality and formulate appropriate mitigation strategies.

In addition to the PM_{10} NES, the Ministry for the Environment issued ambient air quality guidelines (NZAAQG) for air pollutants in 2002 that included a guideline value of 25 μg m^{-3} for particles less than 2.5 μm in aerodynamic diameter ($PM_{2.5}$) (24-hour average). More recently, the World Health Organisation (WHO) has confirmed a $PM_{2.5}$ ambient air quality guideline value of 25 μg m^{-3} (24-hour average) based on the relationship between 24-hour and annual PM concentrations (WHO, 2006). The WHO annual average guideline for $PM_{2.5}$ is 10 μg m^{-3}. These are the lowest levels at which total, cardiopulmonary and lung cancer mortality have been shown to increase with more than 95% confidence in response to exposure to $PM_{2.5}$. The WHO recommends the use of $PM_{2.5}$ guidelines over PM_{10} because epidemiological studies have shown that most of the adverse health effects associated with PM_{10} are from $PM_{2.5}$. The NZAAQG also provides guideline limits for a range of toxic metals and organic compounds that are known to be a health hazard in their own right.

1.2 IDENTIFYING THE SOURCES OF AIRBORNE PARTICLE POLLUTION

Measuring the mass concentration of particulate matter (PM) provides little or no information on the identities of the contributing sources. Airborne particles are composed of many elements and compounds emitted from various sources and a multivariate analysis technique known as receptor modelling allows the determination of relative mass contributions from sources impacting the total PM mass of samples collected at a monitoring site. First, gravimetric mass is measured and then a variety of methods can be used to determine the elements and compounds present in a sample. In this study, elemental concentrations in the samples were determined using inductively coupled plasma mass spectrometry (ICP-MS) for arsenic determination and X-ray fluorescence spectroscopy (XRF) at the New Zealand Ion Beam Analysis facility operated by GNS Science in Lower Hutt.

X-ray fluorescence is a mature analytical technique that provides the non-destructive determination of multi-elemental concentrations in samples. Using elemental concentrations, coupled with appropriate statistical techniques and purpose-designed mathematical models, the sources contributing to each ambient sample can be identified. In general, the more ambient samples that are included in the analysis, the more robust the receptor modelling results. Appendix 1 provides a description of the XRF analytical process and receptor modelling techniques.

1.3 REPORT STRUCTURE

This report is comprised of seven main chapters. Briefly, the remaining chapters have been broken down as follows:

1. Chapter 2 describes the methodology and analytical techniques used for the receptor modelling analysis.
2. Chapter 3 describes the Whangarei ambient air quality monitoring site, temporal trends in PM_{10} concentrations and local meteorology.
3. Chapter 4 presents the PM_{10} compositional analyses and the receptor modelling results including temporal variations and seasonality.
4. Chapter 5 presents trend analyses and discussion.
5. Chapter 6 provides a summary of the research findings and recommendations.

2.0 METHODOLOGY

PM_{10} samples were collected onto glass fibre filters using a high-volume sampler located at the NRC monitoring site on top of the Northland Regional Council office building at Water Street, Whangarei. Figure 2.1 presents the location of the monitoring site. All PM sampling and systems maintenance at the sampling site was carried out by NRC, and as such, NRC maintains all records of equipment, flow rates and sampling methodologies used for the PM sampling regimes. Filter conditioning, weighing and re-weighing for PM_{10} gravimetric mass determinations were carried out by the NRC laboratory in Whangarei.

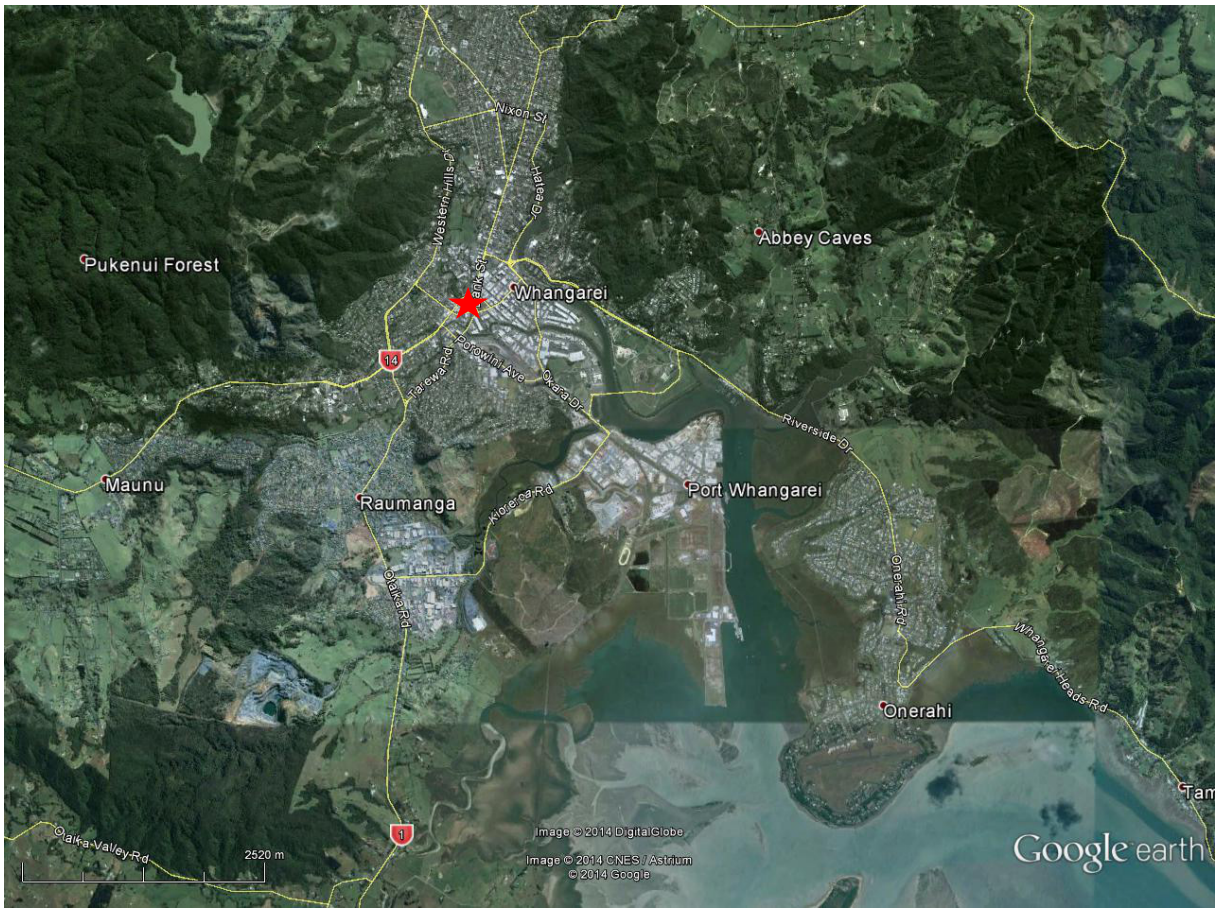

Figure 2.1 Location of the Water Street monitoring site in Whangarei city (★) (source: Google Maps).

Elemental concentrations in PM_{10} were determined using X-ray fluorescence spectroscopy (XRF) at the New Zealand Ion Beam Analysis Facility in Gracefield, Lower Hutt, with additional arsenic determination (for a selection of samples) by ICP-MS performed at Hills Laboratories in Hamilton. Black carbon (BC) concentrations were determined using light reflection techniques. Full descriptions of the analytical and data analysis techniques used in this study are provided in Appendix 1.

The authors visited the monitoring site and noted typical activities occurring in the surrounding area that may contribute to PM concentrations. These observations are reflected in the conceptual receptor model described in Chapter 3.

2.1 DATA ANALYSIS AND REPORTING

The receptor modelling results within this report have been produced in a manner that provides as much information as possible on the relative contributions of sources to PM concentrations so that it may be used for monitoring strategies, air quality management and policy development. The data have been analysed to provide the following outputs:

1. masses of elemental species apportioned to each source;
2. source elemental profiles;
3. average PM_{10} mass apportioned to each source;
4. temporal variations in source mass contributions (timeseries plots);
5. seasonal variations in source mass contributions. For the purposes of this study, summer has been defined as December–February, autumn as March–May, winter as June–August and spring as September–November;
6. analysis of source contributions on peak PM days. Table 2.1 presents the relevant standards, guidelines and targets for PM concentrations.

Table 2.1 Standards, guidelines and targets for PM concentrations.

Particle Size	Averaging Time	Ambient Air Quality Guideline	MfE* 'Acceptable' air quality category	National Environmental Standard
PM_{10}	24 hours	50 µg m^{-3}	33 µg m^{-3}	50 µg m^{-3}
	Annual	20 µg m^{-3}	13 µg m^{-3}	
$PM_{2.5}$	24 hours	25 µg m^{-3}	17 µg m^{-3}	

*Ministry for the Environment air quality categories taken from the Ministry for the Environment, October 1997 – ***Environmental Performance Indicators: Proposals for Air, Fresh Water and Land***.

3.0 WATER STREET MONITORING SITE AND SAMPLING METHODOLOGY

3.1 SITE DESCRIPTION

Size-resolved PM_{10} samples were collected at an ambient air quality monitoring station located on top of the roof of the NRC building at 35 Water Street, Whangarei (Lat: –35.725255; Long: 174.317721°, elevation: 6 m). Figure 3.1 presents the site location on a map of the local area.

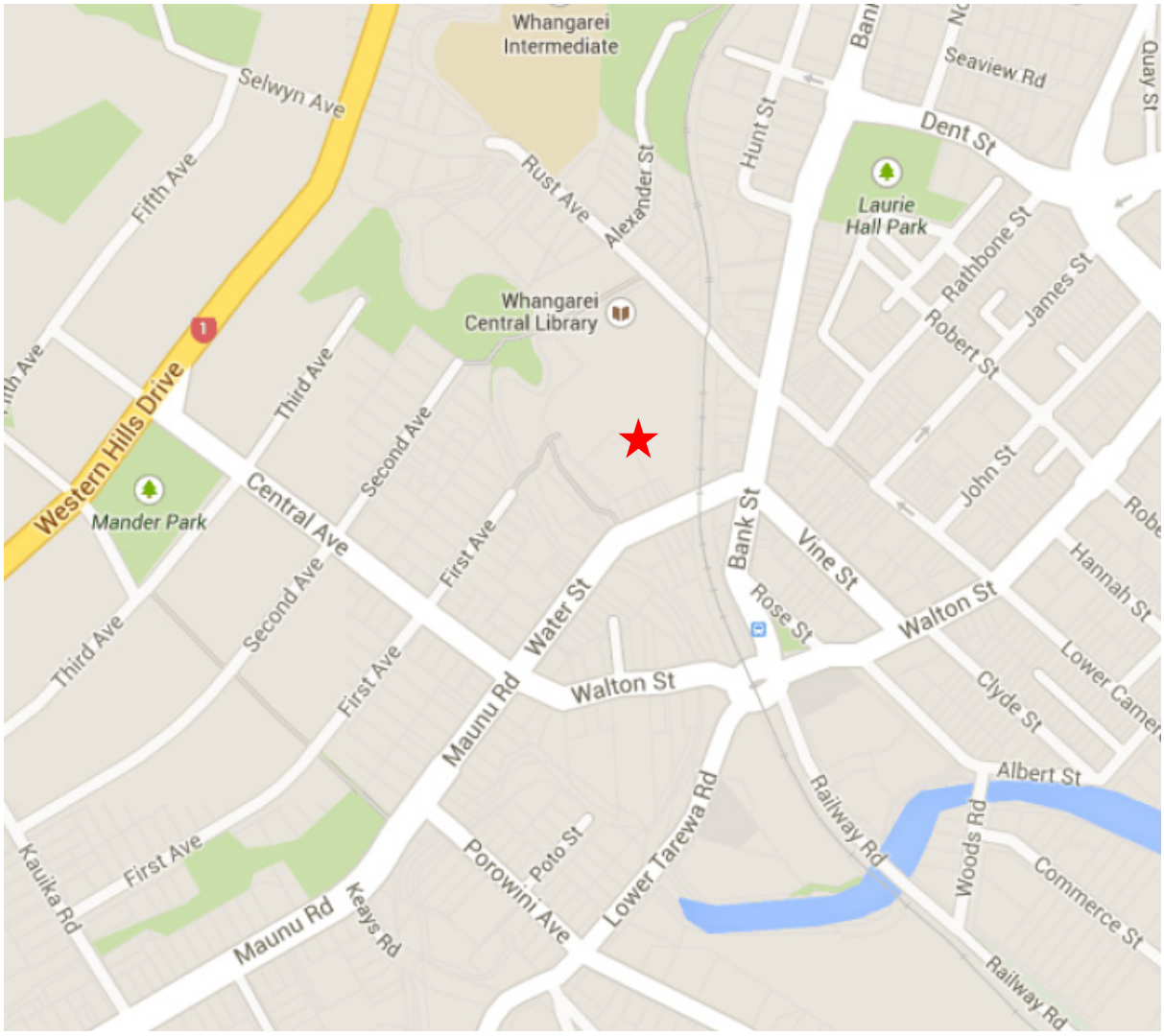

Figure 3.1 Map showing the location of the Water Street monitoring site (★) (source: Wises Maps www.wises.co.nz).

Water Street is located on the northwestern edge of the Whangarei CBD. The site was approximately 50 m from the nearest road and surrounded by open space or buildings no more than two stories high. To the northwest of the site is the Whangarei residential suburb of Avenues with bush clad hills further north and west. To the south and southwest the land opens out into the port area and Whangarei Harbour. The city of Whangarei essentially sits in the confluence of two valleys that drain into the harbour. Figure 3.2 provides an aerial photo of the Water Street monitoring site and its immediate environs and Figure 3.3 shows a photograph of the high-volume sampler located on the roof of the NRC building.

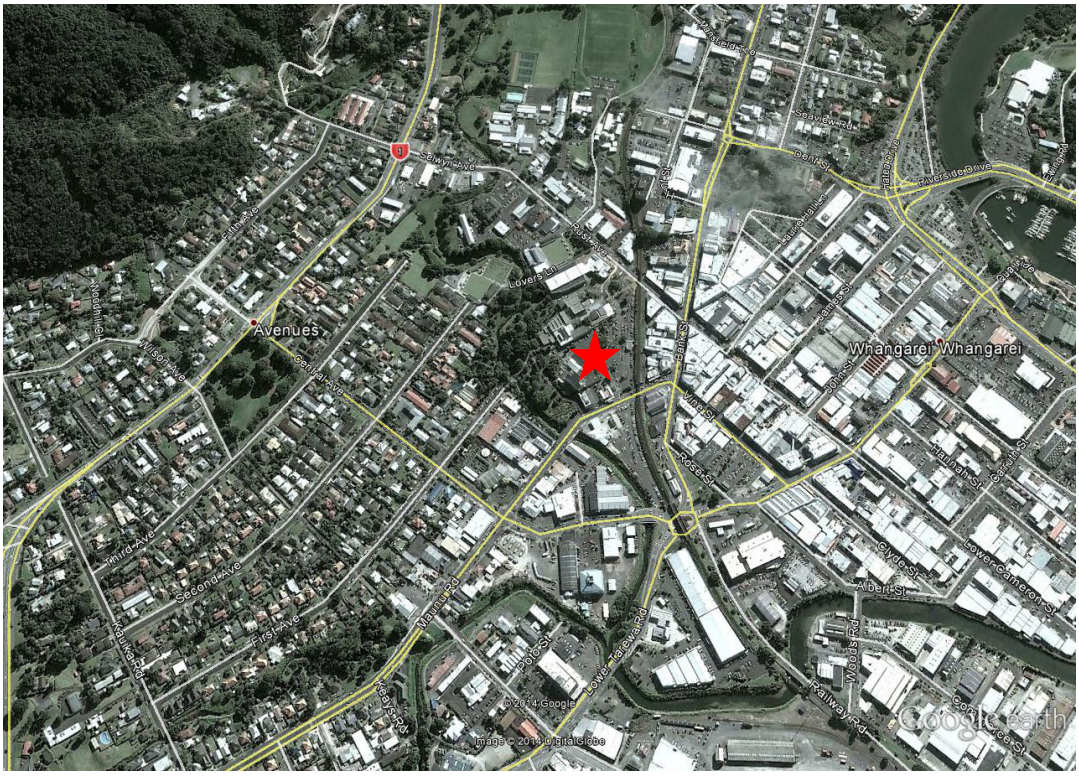

Figure 3.2 Aerial view of the Water Street monitoring site (★) and its immediate environs (from Google Earth).

Figure 3.3 NRC High-volume sampler on the roof of the office building.

3.2 PARTICULATE MATTER SAMPLING AND MONITORING PERIOD

Overall, approximately 450 PM_{10} samples were collected using the high-volume sampler system from September 2004 until January 2012. Samples were collected on a one-day-in-six (midnight to midnight) sampling regime. Mass concentrations of PM_{10} were determined gravimetrically, where a filter of known weight was used to collect the PM samples from a known volume of sampled air. The loaded filters were the re-weighed to obtain the mass of collected PM. The average PM concentration in the sampled air was then calculated.

3.3 CONCEPTUAL RECEPTOR MODEL FOR PM AT WATER STREET

An important part of the receptor modelling process is to formulate a conceptual model of the receptor site. This means understanding and identifying the major sources that may influence ambient PM concentrations at the site. For the Water Street site, the initial conceptual model includes local emission sources:

- Motor vehicles – roads with higher density traffic will dominate
- Commercial activities
- Domestic activities – mainly emissions from solid fuel fires for domestic heating during the winter
- Local wind-blown soil or road dust sources

Longer range sources may also contribute including:

- Marine aerosol
- Secondary particulate (sulphate, nitrate and organic species)
- Industrial emissions (e.g., Marsden Point refinery, fertiliser production)
- Shipping emissions

Another category of emission sources that may contribute are those considered to be 'one-off' emission sources:

- Fireworks displays and other special events (e.g., Guy Fawkes day);
- Short-term road works and demolition/construction activities.

The variety of sources described above can be recognised and accounted for using appropriate data analysis methods such as examination of seasonal differences, temporal variations and receptor modelling itself.

3.4 LOCAL METEOROLOGY AT THE WATER STREET SITE

There was no meteorological monitoring station located at the monitoring site, therefore only a broad assessment of the influence of meteorology on local air pollution was possible using meteorological data from Whangarei airport at Onerahi. The predominant wind directions for Whangarei were from the southwest and northwest, with lesser frequency of winds from the easterly quadrant as shown in Figure 3.4. The meteorology at the Water Street site was likely to be defined and constrained by the local topography because the site was located at the confluence of two valley systems. Seasonality was apparent in wind directions, as shown in Figure 3.5. Strong southwesterly winds tended to dominate during spring and summer, whereas lighter winds from the northwest predominated during autumn (with the highest percentage calms also during this season) and winter than during other seasons.

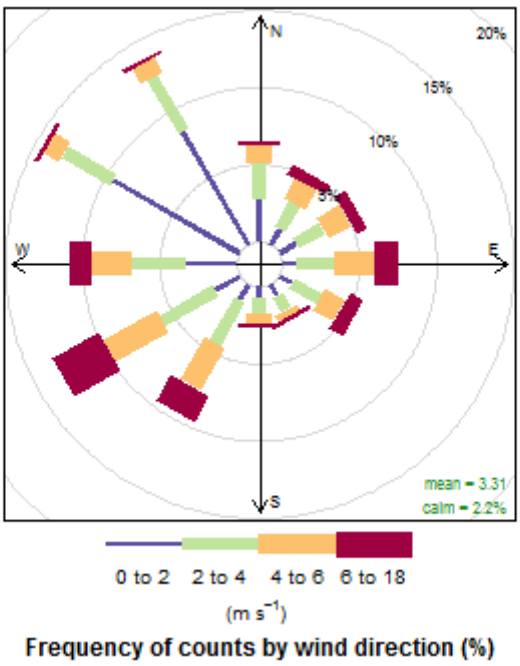

Figure 3.4 Wind rose for entire monitoring period (September 2004–January 2012).

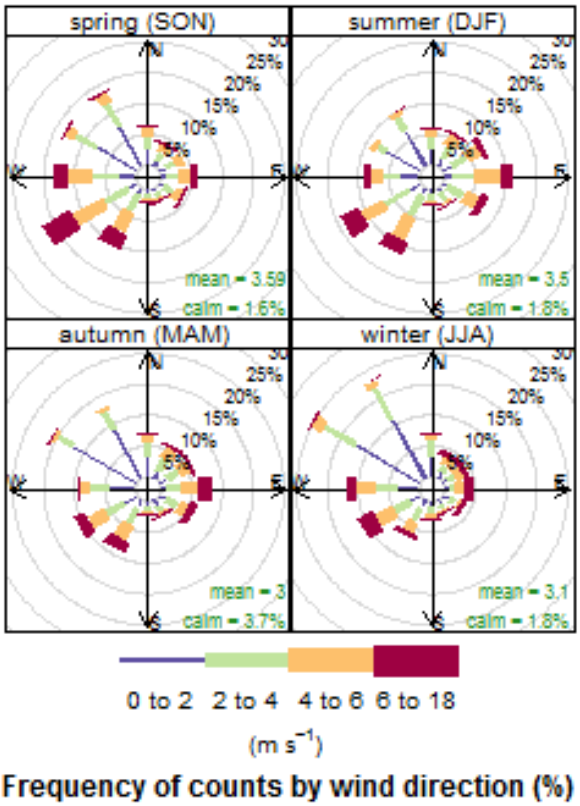

Figure 3.5 Wind roses by season over the entire monitoring period (September 2004–January 2012).

Figure 3.6 presents the average monthly temperature for the monitoring period as recorded at Onerahi. The coolest monthly temperatures were during the winter months.

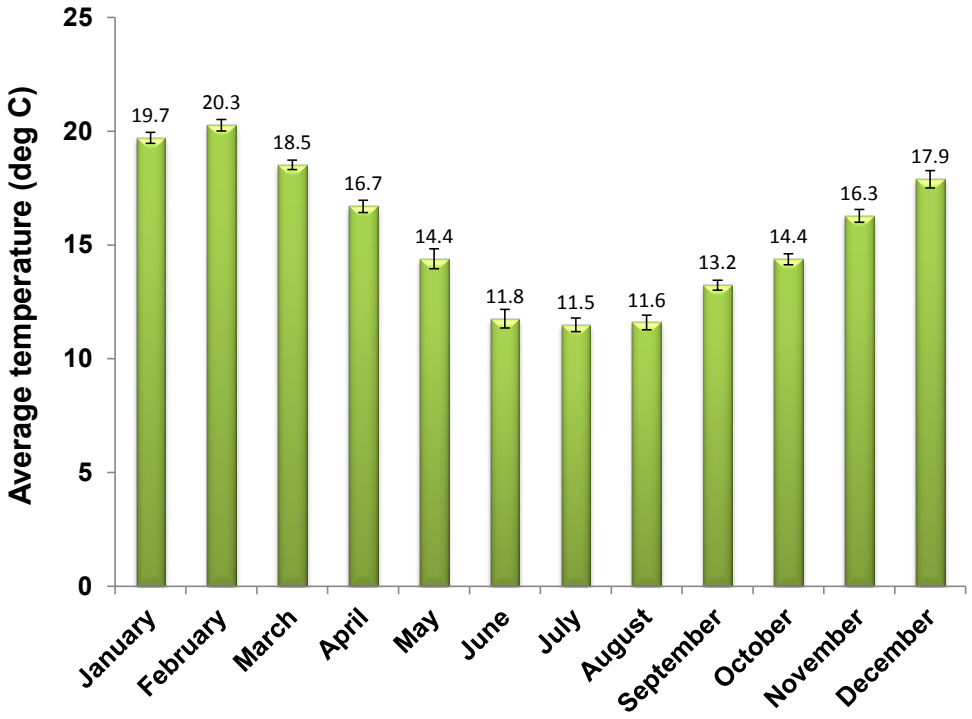

Figure 3.6 Average monthly temperature over the entire monitoring period (September 2004–January 2012).

3.5 PM_{10} CONCENTRATIONS AT THE WATER STREET SITE

The PM_{10} samples from the Water Street site were collected using a high-volume sampler system on a one-day-in-six sampling regime, as discussed in Section 3.2, from September 2004 to January 2012. The gravimetric results for the PM_{10} samples are presented in Figure 3.7. Some seasonal patterns are apparent from Figure 3.7, with PM_{10} concentrations tending to peak during June and July. However, peak PM_{10} concentrations also occurred outside of the winter season, and these are likely to be explained by different sources of particulate matter contributing at different times of the year. The one NESAQ exceedance (PM_{10} > 50 µg m^{-3} 24-hour average), shown in Figure 3.7, was related to an Australian dust storm event on the 25 September 2009 that also resulted in peak concentrations during that period in the Auckland and Waikato regions (Davy et al., 2011). Gaps present in Figure 3.7 resulted from missed sample days or samples removed as part of the quality assurance process.

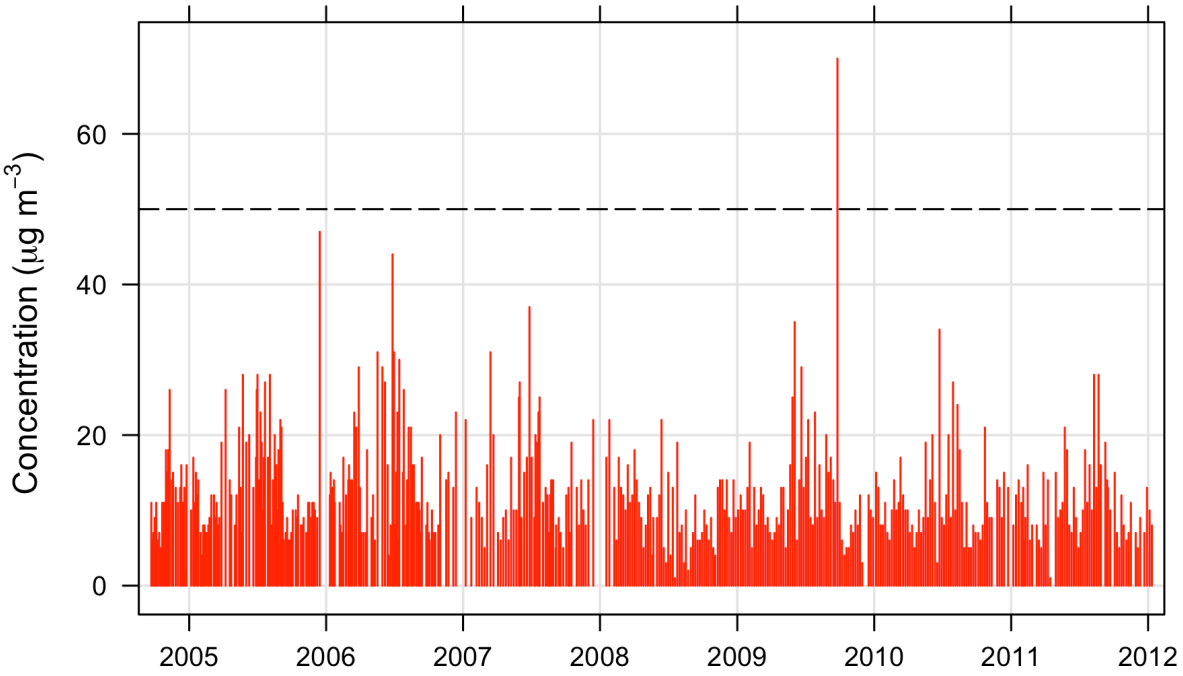

Figure 3.7 Gravimetric PM_{10} results. Gaps are from missed sample days or samples removed as part of the quality assurance process. The hashed line indicates the New Zealand NESAQ for PM_{10} (50 µg m^{-3}).

The variation in average PM_{10} concentrations can be seen when considering monthly and day-of-the-week average concentrations as presented in Figure 3.8.

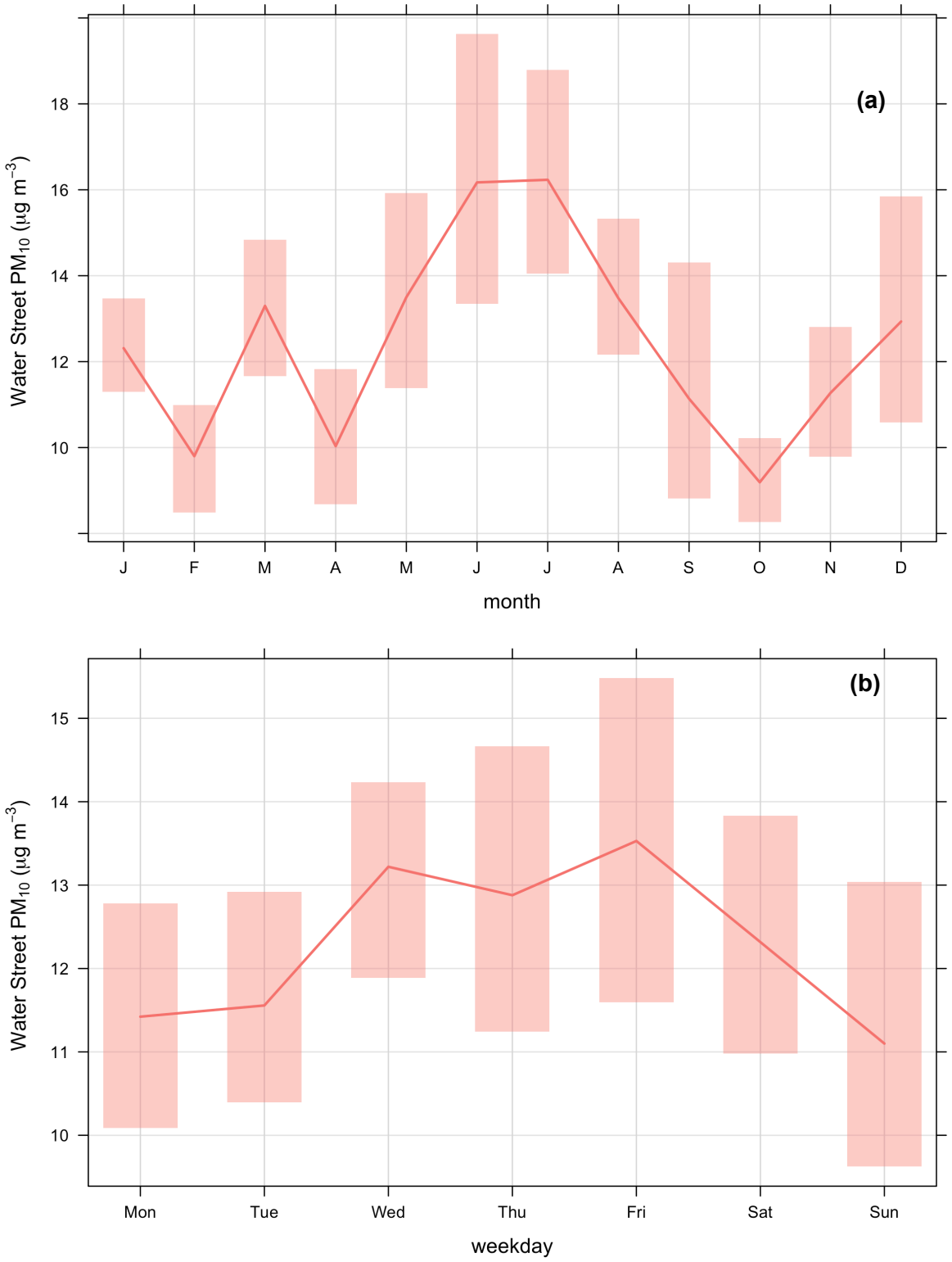

Figure 3.8 PM_{10} concentrations at the Water Street site showing average (and 95% CL) by (a) month and (b) day of the week.

Higher PM_{10} concentrations were observed on week days but were not statistically significant to the 95% confidence interval.

3.6 BLACK CARBON CONCENTRATIONS AT THE WATER STREET SITE

The PM_{10} high-volume glass-fibre filter set was analysed for black carbon (BC) concentrations. Black carbon (BC) has been studied extensively, but it is still not clear to what degree it is elemental carbon (EC (or graphitic), C(0)) or high molecular weight refractory weight organic species or a combination of both (Jacobson et al., 2000). Current literature suggests that BC is likely a combination of both, and that for combustion sources such as petrol and diesel fuelled vehicles, biomass combustion (wood burning) and fossil fuels (coal burning), EC and organic carbon compounds (OC) are the principle aerosol components emitted (Fine et al., 2001, Jacobson et al., 2000, Salma et al., 2004, Watson et al., 2002).

Determination of carbon (soot) on the filters was performed by light reflection to provide the BC concentration. The absorption and reflection of visible light on particles in the atmosphere or collected on filters is dependent on the particle concentration, density, refractive index and size. For atmospheric particles, BC is the most highly absorbing component in the visible light spectrum with very much smaller components coming from soils, sulphates and nitrate (Horvath, 1993, Horvath, 1997). Hence, to the first order it can be assumed that all the absorption on atmospheric filters is from BC. The main sources of atmospheric BC are anthropogenic combustion sources and include biomass burning, motor vehicles and industrial emissions (Cohen et al., 2000). Cohen and co-workers found that BC is typically 10–40% of the fine mass ($PM_{2.5}$) fraction in many urban areas of Australia. Further details on the black carbon measurements a provided in Appendix 1.

The interesting point about BC is that is closely associated with the $PM_{2.5}$ component of PM_{10} and therefore provides an indication of $PM_{2.5}$ concentration patterns and time-series. Figure 3.9 presents the BC concentrations at Water Street.

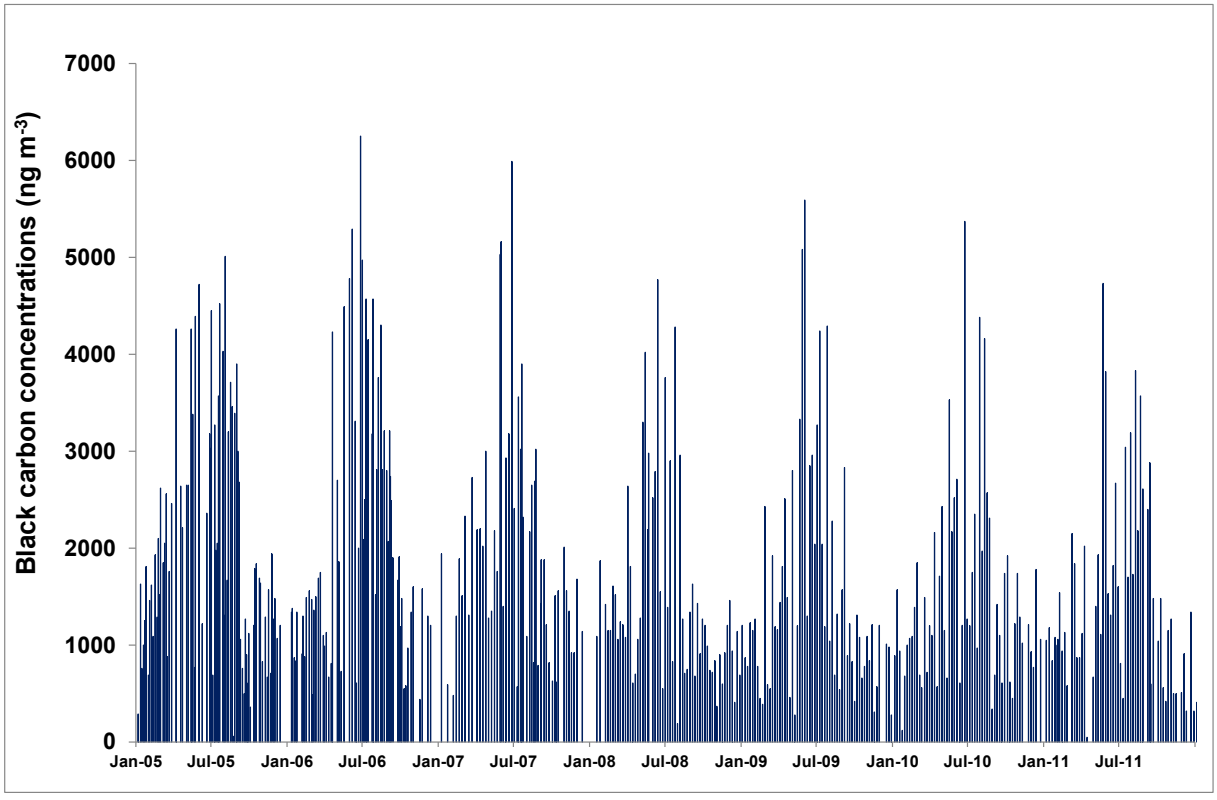

Figure 3.9 Black carbon concentrations at the Water Street site.

Immediately evident from the BC data is the much greater seasonality in BC concentrations at the Water Street site indicating that peak concentrations from combustion sources (and by inference peak combustion source emissions) were likely to occur during the winter in the Whangarei airshed. The variation in average BC concentrations can be seen when considering monthly and day-of-the-week average concentrations as presented in Figure 3.10, which shows that the highest concentrations occurred during the winter and the lowest weekday concentrations occurred on Sunday (statistically significant to 95% confidence limits).

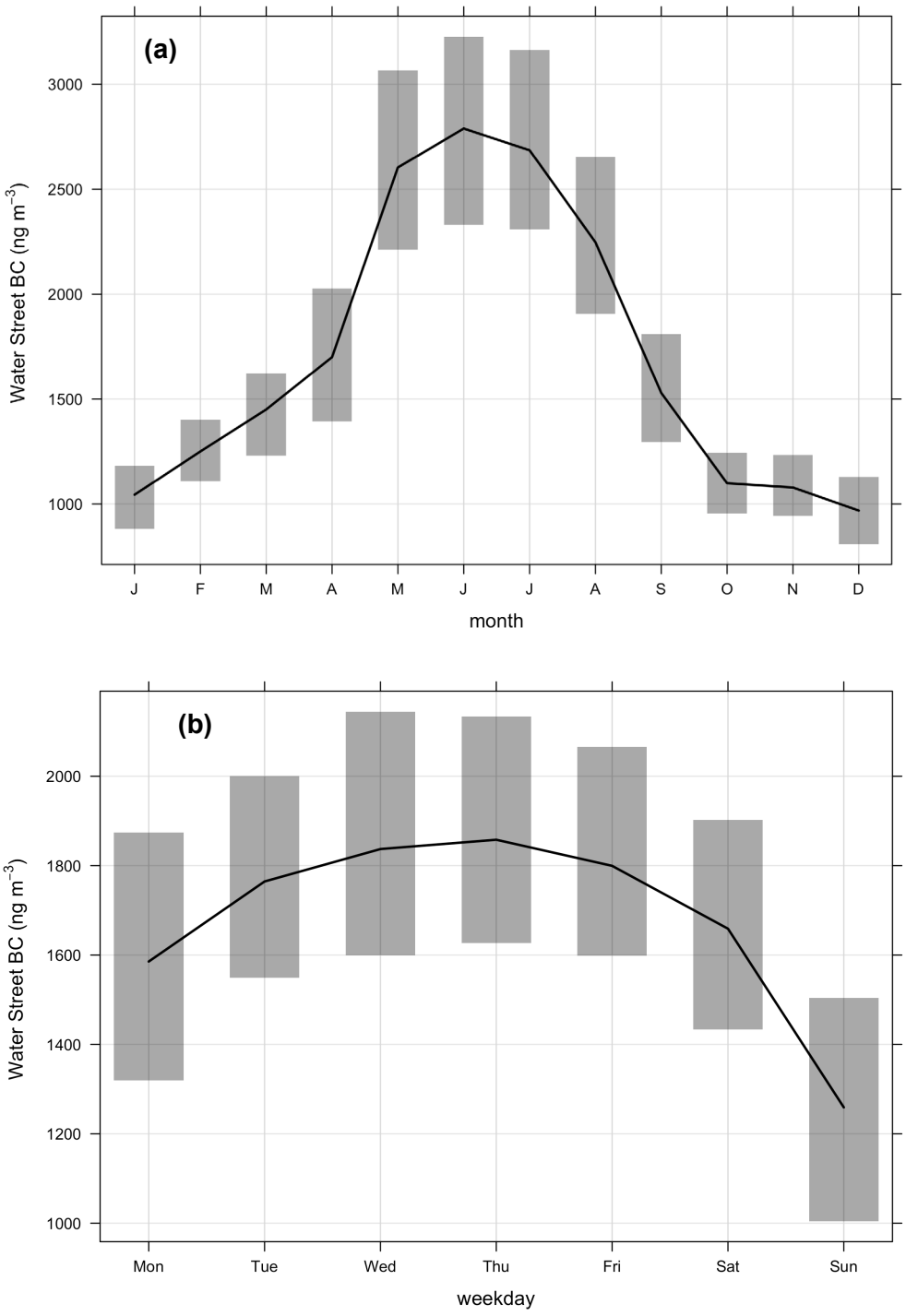

Figure 3.10 BC concentrations at the Water Street site showing average (and 95% CL) by (a) month and (b) day of the week.

This page is intentionally left blank.

4.0 RECEPTOR MODELING ANALYSES FOR PM_{10} AT WATER STREET

4.1 COMPOSITION OF PM_{10} AT WATER STREET

Elemental and black carbon (BC) concentrations in PM_{10} samples were determined using X-ray fluorescence (XRF) and light reflection respectively, the experimental details for which are discussed in detail in Appendix 1. A brief synopsis is presented here. The PM_{10} samples from the Water Street site were collected on glass fibre filter material which is composed primarily of silicon dioxide along with alkali earth metals (Na, Mg, Ca, K). A series of initial experiments were run to identify whether XRF would be a feasible method for quantifying elemental concentrations in the particulate matter collected on glass fibre filters. Ten blank filters were analysed and deviations between the elemental concentrations were investigated. This analysis showed that Na, Mg, K, Al, Si and Ca concentrations in particulate matter could not be determined accurately because they were either part of the composition of the filter matrix, or were present as impurities. For many other elements though, particularly those with atomic numbers equal or higher than titanium, sensible concentration data was able to be extracted. The XRF analytical process includes a reference standard for each element measured. Concentrations and other statistical parameters for elements that were quantified are presented in Table 4.1.

Table 4.1 Elemental concentrations in PM_{10} collected at Water Street.

	Average (ng m^{-3})	Max (ng m^{-3})	Min (ng m^{-3})	Median (ng m^{-3})	StdDev (ng m^{-3})	Ave Uncert (ng m^{-3})	Ave LOD (ng m^{-3})	#>LOD	%>LOD	Signal to Noise ratio
PM_{10} (µg m^{-3})	12	70	1	11	7					
BC	1721	6250	50	1340	1174	344	187	446	99	4
S	44	379	1	32	51	3	3	333	74	18
Cl	303	2924	0	184	328	24	3	448	100	17
Ti	8	284	0	4	15	16	8	135	30	1
V	2	8	0	1	1	4	2	135	30	1
Cr	1	17	0	1	2	3	2	45	10	1
Mn	2	49	0	2	3	4	3	88	20	1
Fe	67	2365	0	28	126	90	52	168	37	1
Ni	2	9	0	2	1	9	6	2	0	1
Cu	2	15	0	1	2	2	1	205	46	1
Zn	6	39	0	5	5	5	4	268	60	1
As	3	18	0	2	3	1	1	279	62	2
Br	2	30	0	1	2	4	2	84	19	1
Cd	2	9	0	1	1	6	3	38	8	1
Sn	3	13	0	2	2	10	4	55	12	1
Sb	4	22	0	2	4	9	4	130	29	1
Cs	7	38	0	6	1	29	12	46	10	1
Ba	31	111	0	27	21	20	16	345	77	1
Pb	12	82	0	8	11	18	12	171	38	1

The other consideration for the XRF analysis was the representativeness of the determined elemental concentrations compared with the bulk sample since the depth penetration of the analytical beam into the filter material is approximately 100-150 microns whereas the glass fibre filters are approximately 500 microns thick. Particulate matter penetration into glass or quartz fibre filters has been found to be around 150–200 microns (Fung et al., 2002). The

feasibility study was able to show that the XRF elemental concentrations were linearly correlated with the bulk concentrations (discussed in Section 4.1.2.). However, due to the glass fibre filter matrix background the analytical data at low concentrations (i.e., from zero to two times the LOD) for many of the elements were still analytically “noisy”. This is quantified by the signal-to-noise-ratio parameter presented in Table 4.1. A ‘strong’ signal-to-noise ratio (s/n > 2) indicates that the element is generally present in concentrations well above the LOD. Smaller or ‘weak’ signal-to-noise ratios (s/n > 2 > 0.2) indicate that the measured elemental concentrations are generally near the detection limit. A ‘bad’ signal-to-noise ratio (s/n < 0.2) is where the element may be present in concentrations near or below the LOD and there is doubt about some of the measurements and/or the error estimates; or the elemental species is only detected some of the time (Paatero and Hopke, 2003).

Figure 4.1 presents a box and whisker plot of the Water Street XRF data presented in Table 4.1. The bottom and top of each box mark the 25th and 75th percentile values respectively. The median value (50th percentile) is marked by the line within the box. The whiskers extend to 1.5 times the inter-quartile range (1.5 times the difference between the 75th and 25th percentile values). Any data outside that range is marked with a red dot.

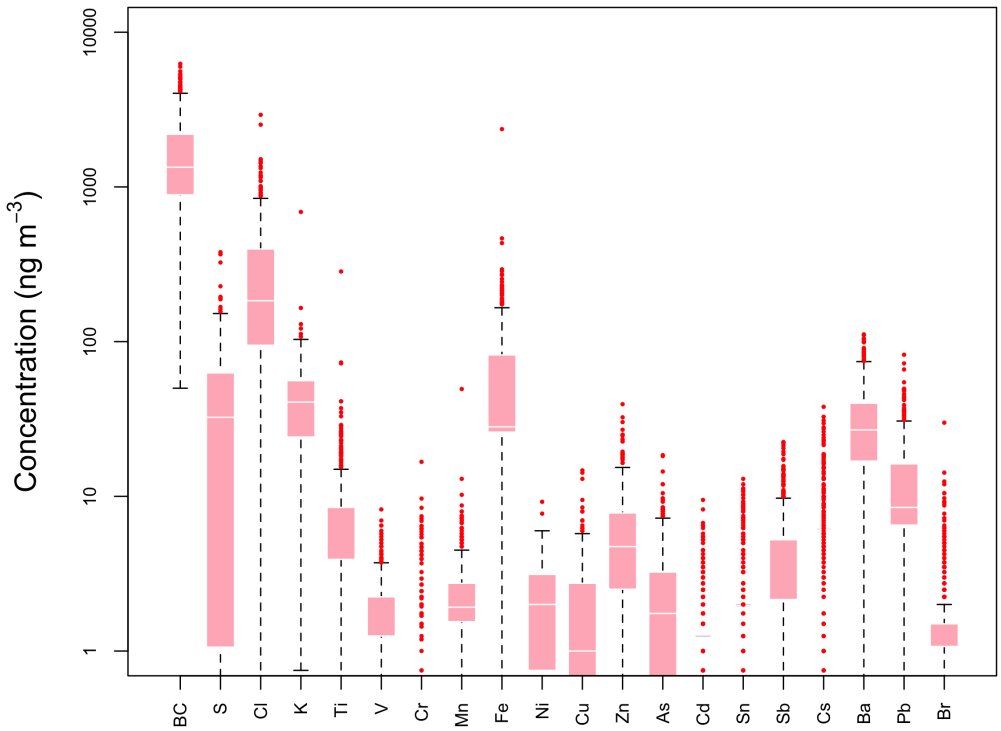

Figure 4.1 Box and whisker plot of XRF elemental data from Water Street.

Interestingly, both arsenic and lead were detected by XRF in a significant number of the particulate matter samples and both elements showed similar time series with winter peaks as presented in Figure 4.2 and Figure 4.3 respectively.

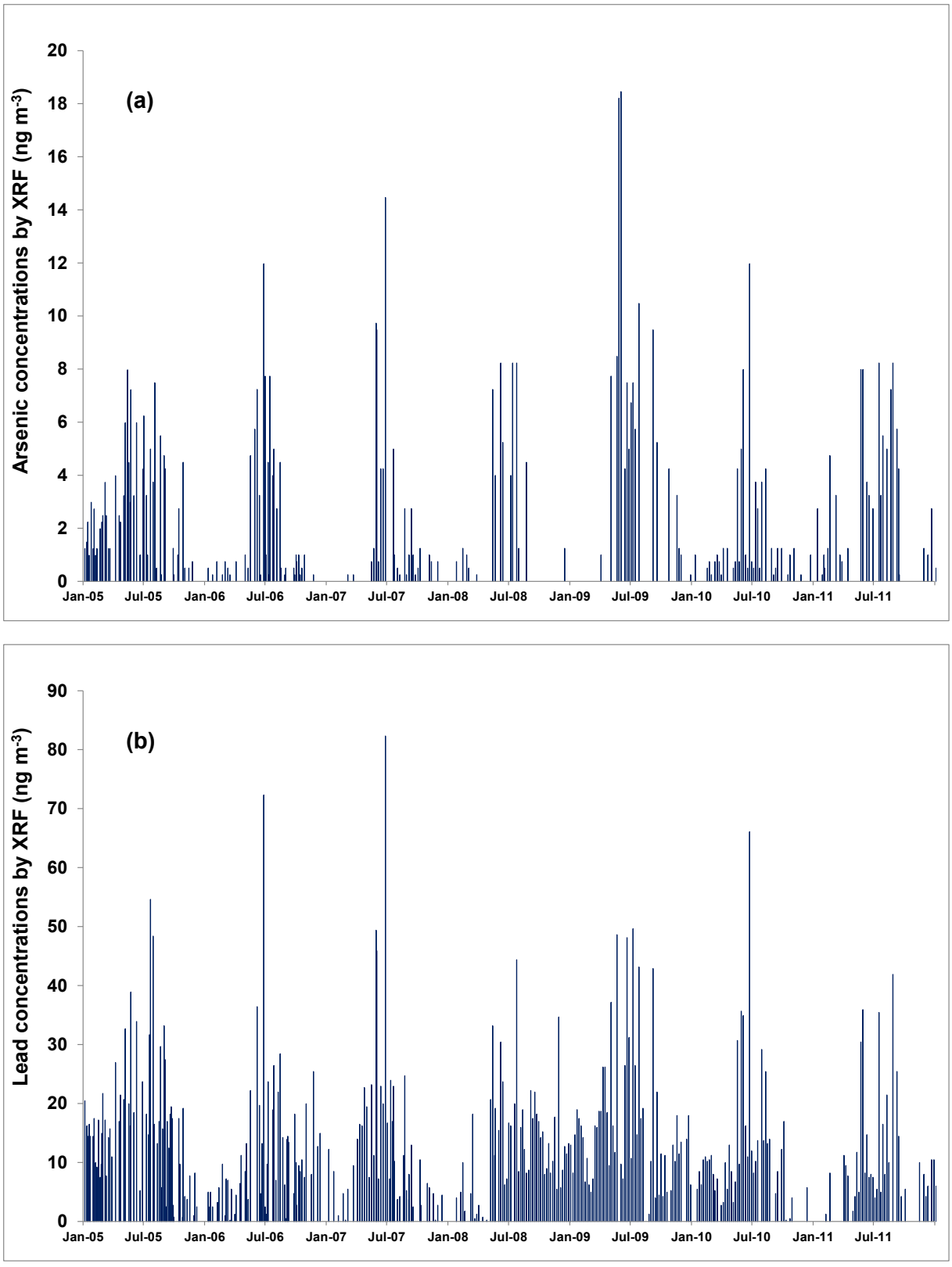

Figure 4.2 (a) Arsenic concentrations and (b) Lead concentrations by XRF for the Water Street site.

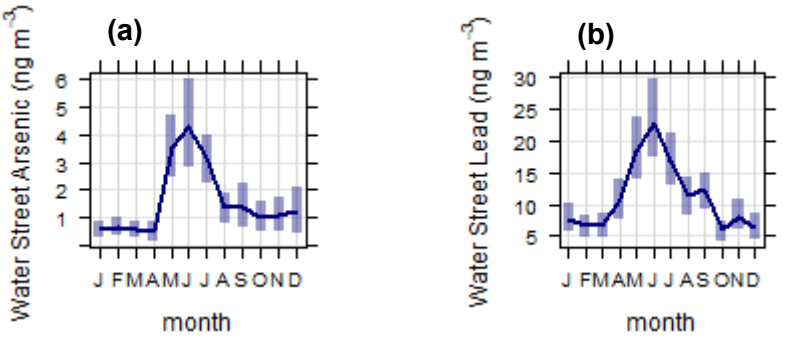

Figure 4.3 (a) Monthly average arsenic concentrations and (b) Monthly average lead concentrations by XRF for the Water Street site.

4.1.1 Arsenic and lead associated with airborne particulate matter

4.1.1.1 Sources of arsenic and lead in the environment

Arsenic and lead occur naturally in many soils and parent rock in New Zealand, with arsenic concentrations typically in the 2 to 6 ppm range although this can be considerably more (50 ppm) in geothermal zones (Craw et al., 2000, Simmons and Browne, 2000, Craw et al., 2003, Robinson et al., 2004). Lead concentrations in New Zealand soils have been found to range from 6 to 16 ppm (Longhurst et al., 2004). Other sources of arsenic and lead in the New Zealand environment are primarily anthropogenic in origin. Arsenic, for example originates from timber treatment and use of treated timber, pesticides, herbicides, fertilisers and mining operations (gold, coal) (Robinson et al., 2004). Lead on the other hand was historically used in paints, as a petrol additive and in agrochemicals. Lead is still used in automotive batteries and some industries and so finds its way into the environment through waste streams such as landfills and wastewater treatment facilities (biosolids).

4.1.1.2 Arsenic, lead and air pollution

Arsenic associated with air particulate matter pollution is primarily due the combustion of arsenic containing fuels such as coal and copper chrome arsenate (CCA) treated timber. Research on emissions from coal fired power plants indicates that arsenic is released as particle associated arsenic oxides, mostly as the fully oxidised arsenate (As in +5 oxidation state) (Shah et al., 2006). Combustion of treated timber in wood burners (or open burning) is at lower temperatures (with a certain amount of pyrolysis) compared to coal fired power plants. Previous analysis suggests both +3 and +4 oxide states are released and that low temperature pyrolosis (< 327 °C) may retain arsenic in the ash (Helsen and van den Bulck, 2003). It has also been shown that the copper and chrome components are preferentially retained in the ash during combustion of CCA treated timber.

Following the phasing out of leaded petrol in 1996, ambient lead concentrations in urban areas have dropped away to background levels though there can be localised effects from the removal of old leaded paint from structures (MfE, 2002). Lead associated with particulate matter will occur in locations where wood that has been painted with leaded paints is used as fuel in fires.

4.1.1.3 Air quality guidelines for arsenic and lead

The New Zealand Ambient Air Quality Guidelines (NZAAQG) contain inhalation based health risk guidelines for arsenic species (MfE, 2002). The guideline value for inorganic arsenic is 0.0055 μg/m^3 (annual average), and for arsine (AsH_3) the guideline value is 0.055 μg/m^3 (annual average). At temperatures above 230 °C arsine decomposes to arsenic oxides (Lide, 1992), therefore arsine is unlikely to be present in combustion emissions. For the purposes of this discussion we assume that arsenic emitted from combustion processes is present as inorganic oxides. The NZAAQG recommend determination of arsenic by PM_{10} sampling in accordance with 40 CFR Part 50, Appendix J (i.e., high-volume sampling), followed by analysis using atomic absorption spectroscopy or an equivalent method.

The NZAAQG for lead in PM_{10} is 0.2 μg m^{-3} (3-month moving average, calculated monthly) with the recommended determination of lead by PM_{10} sampling in accordance with 40 CFR Part 50, Appendix J (i.e., high-volume sampling), followed by analysis using atomic absorption spectroscopy or an equivalent method.

4.1.2 Comparison of XRF arsenic concentrations with standard methodology

Arsenic concentrations in a selected subset of the PM_{10} filters were also measured by inductively coupled plasma mass spectroscopy (ICP-MS) which is considered an equivalent standard methodology for the determination of arsenic for comparison with the NZAAQG values. Essentially the ICP-MS arsenic analyses involved acid digestion of a filter element (47mm punch taken from the filter) followed by ICP-MS determination against standard arsenic solutions.

Filter samples chosen for ICP-MS analysis of As included all winter samples and complete sets of samples for 2006, 2009 and 2011 so that annual averages could be calculated for these years and compared to the NZAAQG. Figure 4.4 presents the arsenic results by ICP-MS.

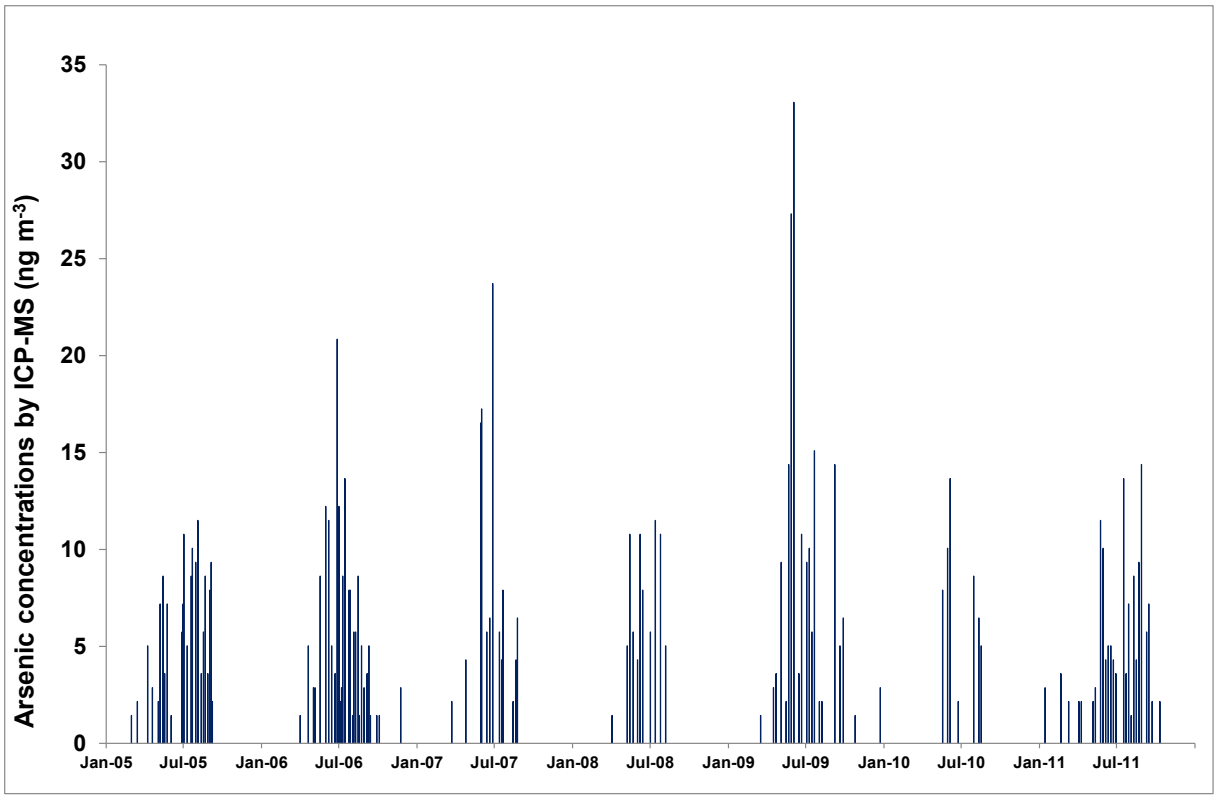

Figure 4.4 Arsenic concentrations in selected samples by ICP-MS for the Water Street site.

The annual average arsenic concentrations for 2006, 2009 and 2011 are presented in Table 4.2. These results indicate that arsenic did not exceed the NZAAQG value as measured at the Water Street site. However, consideration needs to be given to exactly where the As emissions occur and what source the As contamination arises from. Further discussion and analyses of the source of arsenic is provided in Section 4.2.

Table 4.2 Annual average arsenic concentrations in PM_{10} collected at Water Street.

Year	2006	2009	2011
Annual Average ($ng\ m^{-3}$)	2.8	3.1	2.6
Winter Average ($ng\ m^{-3}$)	6.2	7.6	5.6
NZAAQG: 5.5 $ng\ m^{-3}$ (annual average)			

When the ICP-MS As results were compared with the XRF elemental data it was found that the relationship was linear with the slope showing that XRF accounted for 64% of the bulk As concentrations as determined using ICP-MS (Figure 4.5). The analytical results also indicated that the ICP-MS and XRF analytical methods gave a similar detection limit for arsenic in air particulate matter of approximately 1.5 ng m^{-3} (analytical equivalents).

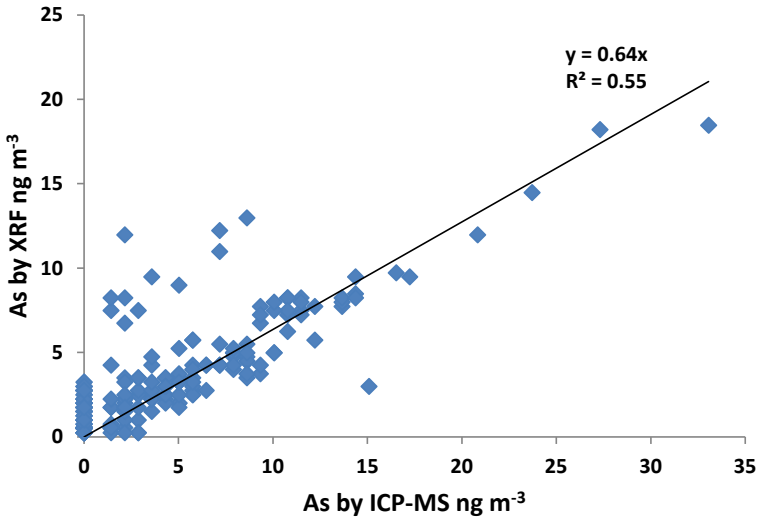

Figure 4.5 Plot showing the relationship between Arsenic concentrations in selected samples determined by ICP-MS and XRF for the Water Street site.

As discussed in Section 4.1 one of the considerations for the XRF analysis was the representativeness of the determined elemental concentrations compared with the bulk sample since the depth penetration of the analytical beam into the filter material is approximately 100–150 microns whereas the glass fibre filters are approximately 500 microns thick. Particulate matter penetration into glass or quartz fibre filters has been found to be around 150–200 microns (Fung et al., 2002). The arsenic analytical results indicated that there was sufficient comparability and linearity with standard a methodology. There were clear time-series evident for a range of elements with concentrations above the limit of detection as determined by XRF analysis to proceed with a source apportionment analysis of the Water Street samples.

4.2 SOURCE CONTRIBUTIONS TO PM_{10} AT WATER STREET

Four source contributors were identified from PMF receptor modelling analyses of the PM_{10} elemental data from Water Street. The elements included in the analyses were based on the diagnostic criteria provided as part of the modelling, the most critical being the signal-to-noise (s/n) ratio. A low s/n ratio indicates that most of the data is near or below the limit of detection, was analytically 'noisy' and therefore unlikely to provide any useful signal for the multi-linear regression (i.e., relationship with other elemental species). Those species with low s/n ratios and were therefore excluded from the process. A full description of the receptor modelling process and model diagnostic outputs are provided in Appendix 3. Figure 4.6 presents the source profiles extracted from the PMF analyses of PM_{10} elemental concentrations. The sources have been identified based on the chemical composition of their profiles and comparison with measured source emission profiles and the results from receptor modelling studies undertaken elsewhere in New Zealand and overseas.

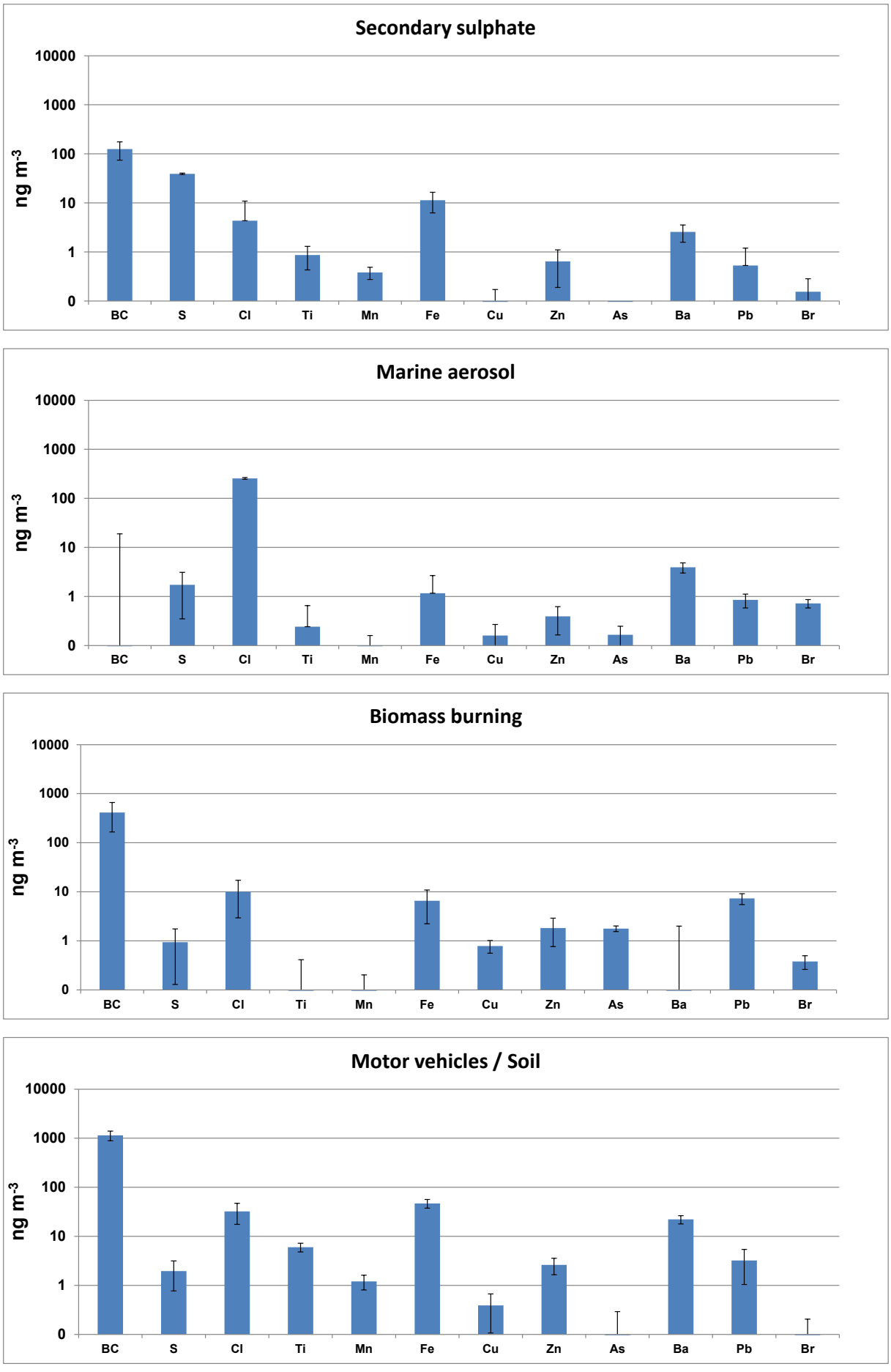

Figure 4.6 Elemental profiles for sources contributing to PM_{10} at Water Street.

The sources identified as contributing significantly to PM_{10} at Water Street were:

1. Marine aerosol: Identified as a marine aerosol (seasalt) source because of the predominance Cl in the profile.
2. Sulphate: This source contribution was from secondary sulphate aerosol because of the dominance of sulphur in the profile.
3. The third factor is due to biomass combustion (representing residential wood burning) and contains BC as the primary species along with Fe, Zn, As, Ba and Pb. Interestingly both arsenic and lead were strongly associated with the biomass combustion profile suggesting that residents are burning copper chrome arsenate (CCA) treated timber and possibly timber painted with lead containing paints in their domestic solid fuel heaters.
4. Motor vehicles/Soil: A combination of motor vehicle emissions and crustal matter (soil) due to the presence of BC, Ti, Mn, Fe, Cu, Zn and Ba as significant components representing a combination of tailpipe emissions, re-entrained road dust and wind-blown soil. The copper present in the profile also indicates emissions from the wear of brake linings.

The source contributors identified in Figure 4.6 were found to explain 83% of the PM_{10} gravimetric mass. The scatter evident in the linear association (r^2 = 0.61) for the predicted (modelled) mass versus observed (gravimetric) mass as presented in Figure 4.7 is most likely an artefact of the uncertainty in PM_{10} gravimetric mass and the relationship between the XRF measured elemental mass and the total mass trapped on the filter as discussed in Section 4.1.2.

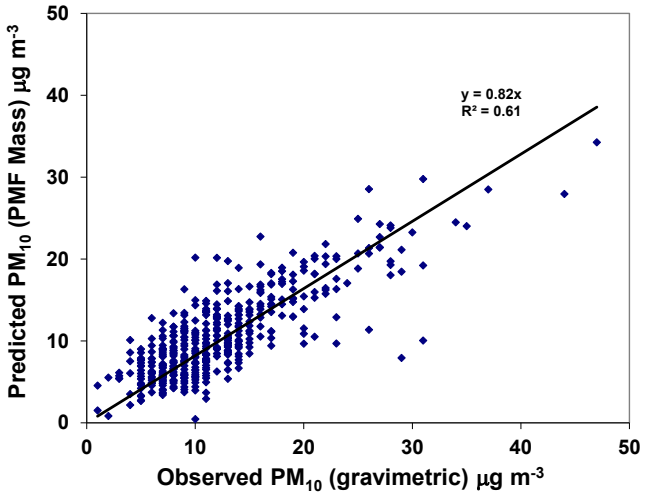

Figure 4.7 Comparison of modelled versus PM_{10} gravimetric mass at Water Street.

Figure 4.8 presents the relative source contributions to PM_{10} at Water Street. Also included in Figure 4.8 are the standard deviations in mass contributions for each of the sources, indicating the variability in average mass contributions over the monitoring period.

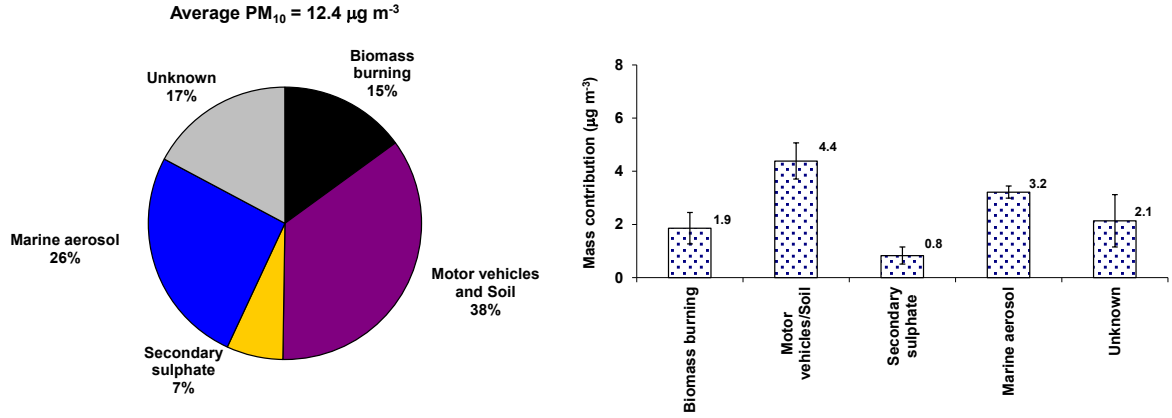

Figure 4.8 Average (2004–2012) relative source contributions to PM_{10} at Water Street.

The average PM_{10} source contributions estimated by PMF indicated that the motor vehicle/crustal matter and marine aerosol sources were the most significant contributor to PM_{10} mass (38% and 33% respectively), with lesser contributions from biomass burning (18%) and secondary sulphate (8%). The unassigned PM_{10} mass ('Unknown') has also been included for reference.

The results of compositional analysis and receptor modelling studies elsewhere in New Zealand would suggest that the marine aerosol and secondary sulphate contributions may be somewhat underestimated. The marine aerosol contribution to PM_{10} in Auckland and Wellington was found to be in the range 6–7 µg m^{-3} and at South Island locations the concentration range was 3–5 µg m^{-3} as long-term averages. Similarly for secondary sulphate the long-term average contribution to PM_{10} across New Zealand is in the order of 1.0–1.5 µg m^{-3}. If the true contributions to PM_{10} from these two sources were similar for the Whangarei context then this may be the most likely explanation for the unaccounted PM_{10} mass at Water Street (2.1 ± 1.0 µg m^{-3}). However, as there is no prior knowledge for expected elemental concentrations and source contributions for Whangarei, care must be taken before any assumptions are made. For the purposes of this study the relative contributions from each source should be considered indicative. However, the source profiles shown in Figure 4.6 and the temporal variation in the PM_{10} source contributions as presented in Figure 4.9 are considered to be strongly representative of the identified sources.

It is evident that PM_{10} mass is dominated by the biomass combustion source during winter, which arises primarily from solid fuel (wood burning) fire emissions used for domestic heating. During other time periods, motor vehicle and soil contributions were the primary source of particulate matter at the Water Street site.

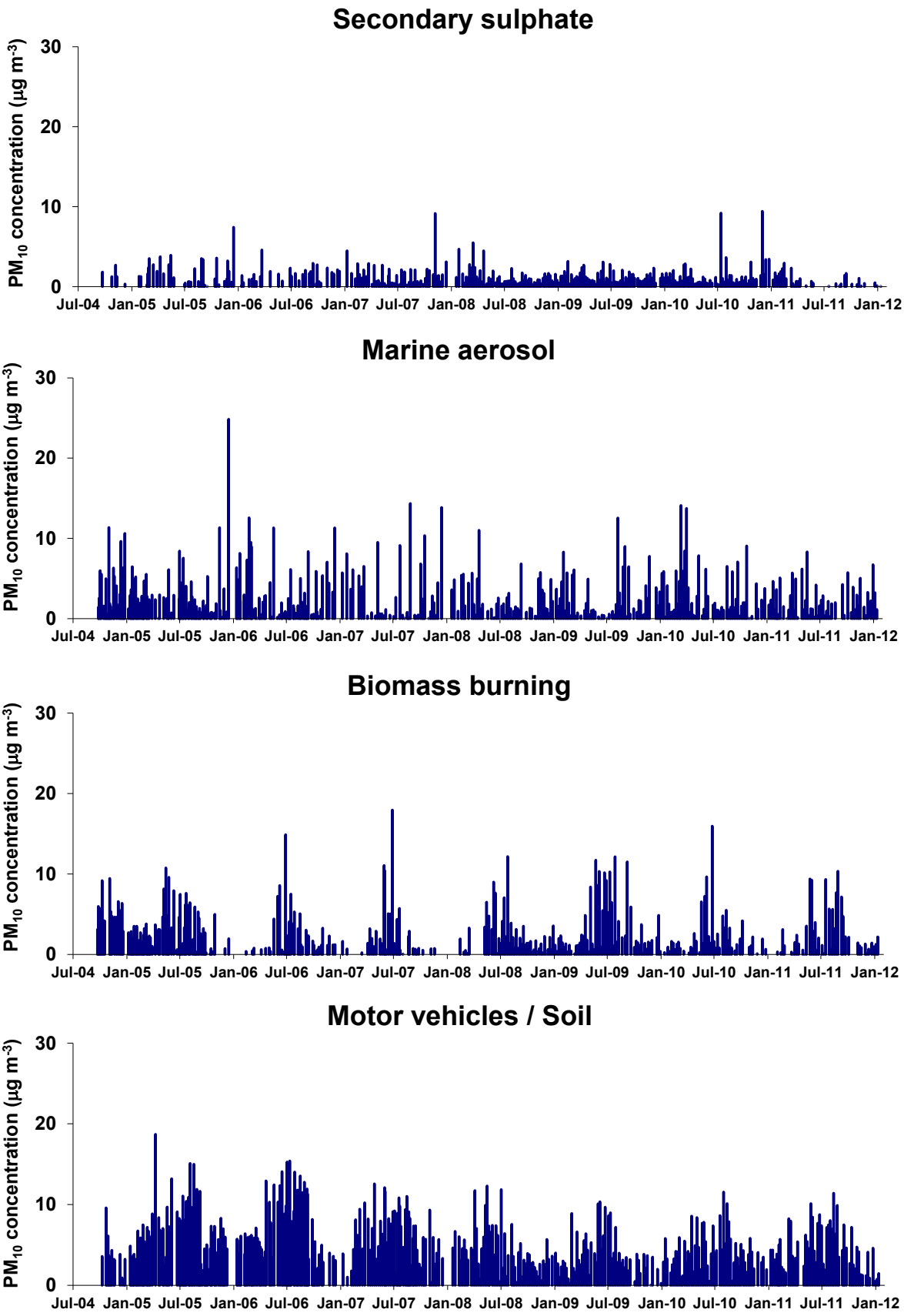

Figure 4.9 Temporal variations in relative source contributions to PM_{10} mass at Water Street.

Note that for the receptor modelling analysis the PM_{10} sample (70 µg m^{-3}) collected 25 September 2009 during the Australian dust storm event (see Section 4.2.1) was removed from the dataset as the unusually high concentrations for some elements (associated with crustal matter) had a disproportionate influence on the receptor modelling results. Quite often this is the case for 'one-off' events, especially for pyrotechnics (fireworks) related emissions of particulate matter due to their strong elemental signatures.

4.2.1 September 2009 Australian dust storm

A severe dust storm originating in the southern lake Eyre Basin between Tinga Tingana and Broken Hill, central Australia (Figure 4.10), swept across the Australian states of New South Wales and Queensland between 22 and 24 September 2009 (Li et al., 2010). The capital, Canberra, experienced the dust storm on 22 September and on 23 September the storm reached Sydney and Brisbane.

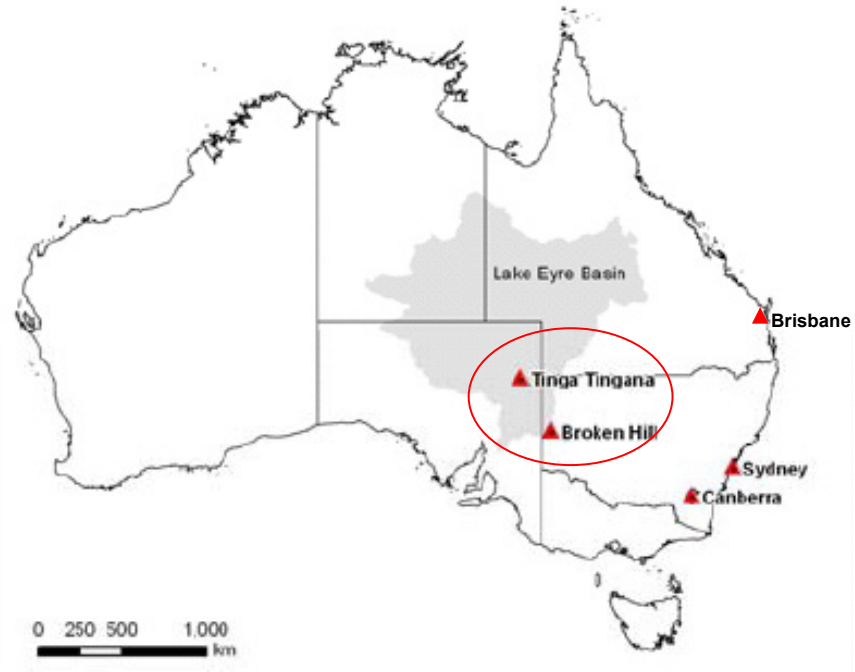

Figure 4.10 Origin of September 2009 eastern Australian dust storm (adapted from (Li et al., 2010))

By 23 September, analysis using MODIS at NASA measured the distance from the northern edge in North Queensland to the southern edge of the plume in NSW to be 2,000 km long and 500 km wide with at least 3 million tonnes of dust estimated to be aloft (Li et al., 2010). The dust plume was then swept across the Tasman Sea by westerly winds as shown by the satellite image in Figure 4.11 and began to impact across the upper North Island of New Zealand.

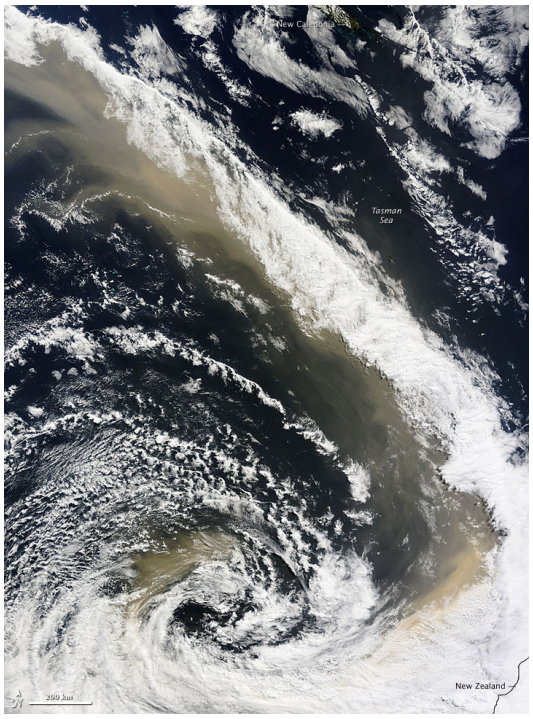

Figure 4.11 Satellite image of 23 September 2009 showing the Australian dust storm out over the Tasman Sea (from http://rapidfire.sci.gsfc.nasa.gov/)

Figure 4.12 presents the measured elemental concentrations measured in the PM_{10} sample collected at Water Street on 25 September 2009.

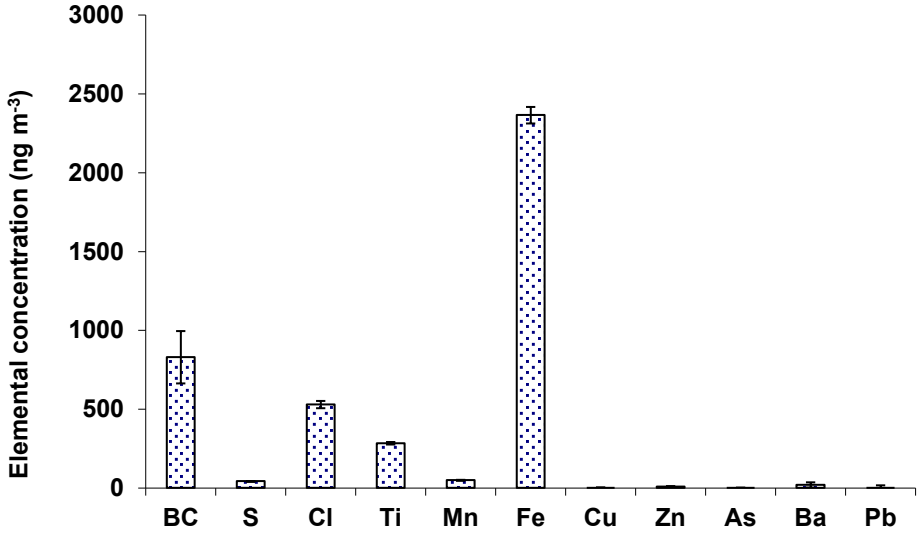

Figure 4.12 Elemental concentrations for the PM_{10} sample (70 µg m^{-3}) collected at Water Street on 25 September 2009 during an Australian dust storm event.

The sample collected on 25 September 2009 contained the highest elemental concentrations of Ti, Mn and Fe (as the primary indicators of crustal matter) for the entire monitoring period. As a comparison Figure 4.13 presents elemental concentration data from five monitoring sites in Auckland City that captured the same dust event. The Khyber Pass Road, Takapuna, Henderson, Penrose and Queen Street sites captured the beginning of the event on 24 September 2009 (all sites recorded PM_{10} concentrations at around 40 µg m^{-3}), while the Queen street site also sampled on 25 September 2009 with the highest concentration recorded (PM_{10} = 130 µg m^{-3}) when the bulk of the Australian dust was swept across New Zealand.

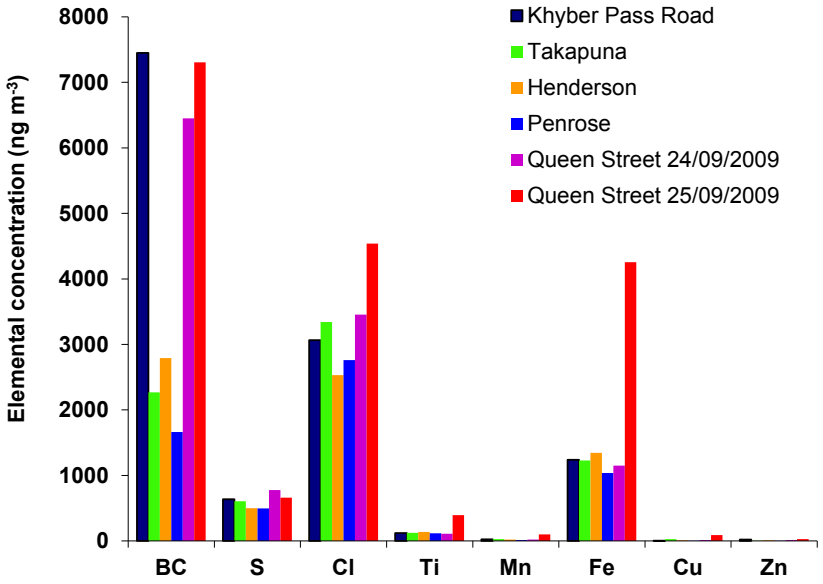

Figure 4.13 Elemental concentrations for PM_{10} samples (70 µg m^{-3}) collected at Auckland monitoring sites on 24 and 25 September 2009 during an Australian dust storm event.

When the elemental ratios for Ti, Mn and Fe in the samples were compared for all sites (Northland and Auckland, they were found to be very similar (Table 4.3) indicating a single originating source.

Table 4.3 Elemental ratios for Ti and Mn relative to Fe at Water Street and Auckland city sites.

Site	Fe/Ti	Fe/Mn
Water Street (25/09/2009)	8.3	47.9
Khyber Pass Road (24/09/2009)	10.1	48.3
Takapuna (24/09/2009)	10.0	42.1
Henderson (24/09/2009)	9.6	58.5
Penrose (24/09/2009)	8.8	64.4
Queen Street (24/09/2009)	10.4	53.9
Queen Street (25/09/2009)	10.8	42.8

A scanning electron microscopy image of the Water Street sample collected on 25 September 2009 is presented in Figure 4.14 showing that the particles were 2–10 μm in diameter with the morphology of crustal matter aerosol.

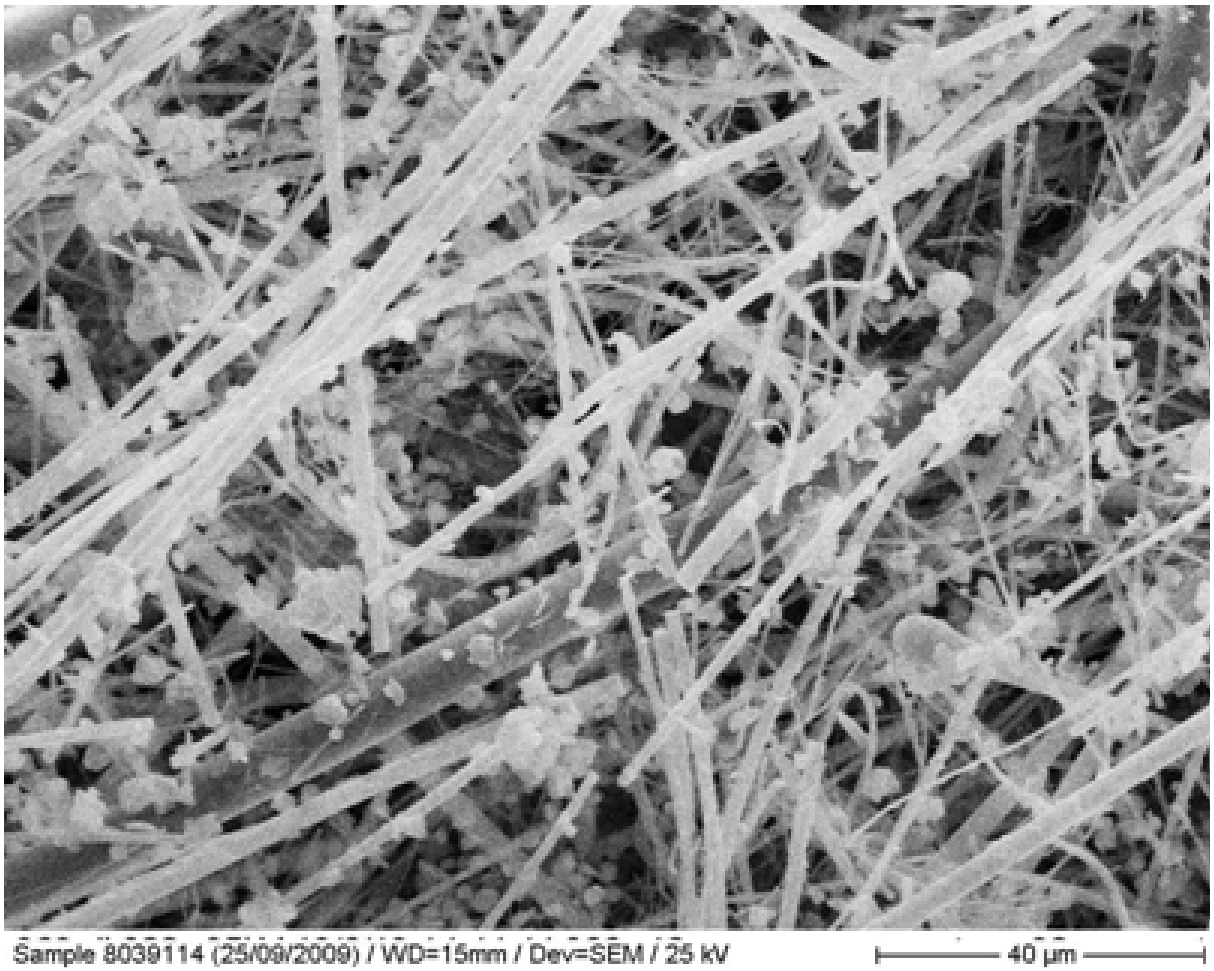

Figure 4.14 Scanning electron microscope image for the PM_{10} sample (70 μg m^{-3}) collected at Water Street on 25 September 2009 during an Australian dust storm event (the long fibres are the glass filter matrix.

4.3 SEASONAL VARIATIONS IN PM_{10} AT WATER STREET

The primary source of PM_{10} during the winter (June–August) at Water Street was biomass combustion associated with solid fuel fire emissions for domestic heating as presented in Figure 4.15. The marine aerosol PM_{10} and secondary sulphate sources showed some seasonality, with higher contributions during the spring and summer. The combined motor vehicle and crustal matter source seasonal variations reflect the higher contribution from wind-blown soil during the drier summer months (December–January).

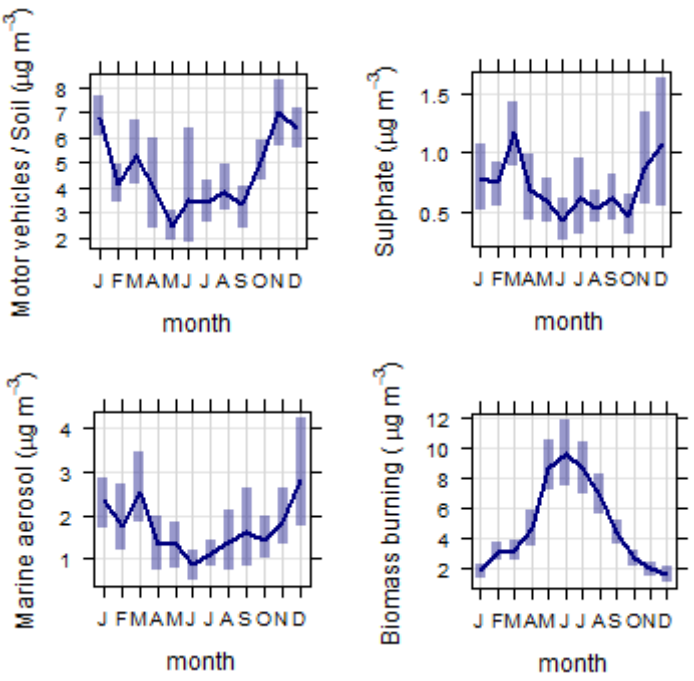

Figure 4.15 2004–2012 seasonal variations in PM_{10} source contributions at Water Street (the shaded bars are the 95% confidence intervals).

Sources of secondary sulphate are likely include emissions from shipping activities in the port area (Davy et al., 2008) and industrial emissions. Longer range sources include marine phytoplankton activity (release of dimethyl sulphide as a gaseous precursor to secondary sulphate) and potentially and emissions of SO_2 gas from geothermal activity (Davy et al., 2009b). Analysis of temporal and seasonal variations in marine aerosol showed higher concentrations during spring and summer, indicating that the generation of marine aerosol is dependent on meteorological factors, such as wind and evaporation potential.

5.0 TREND ANALYSIS FOR PARTICULATE MATTER AT WATER STREET

5.1 TRENDS IN PM_{10} CONCENTRATIONS

The analysis of trends in air pollutant concentrations is critical for assessing source activity and the effects of pollution mitigation strategies and policy intervention measures to reduce air pollution concentrations. The 8-year PM_{10} dataset from Water Street provides the opportunity to examine trends in PM_{10} over the 2004–2012 time period.

The openair package based on 'R' statistical software has been used to analyse the Whangarei data for trends (Carslaw, 2012, Carslaw and Ropkins, 2012, Team, 2011). For the trend analysis, the TheilSen function in openair was used (Carslaw, 2012). The analysis of trends in the PM_{10} concentration data shows that year-on-year PM_{10} concentrations are decreasing by 0.5 µg m^{-3} (Figure 5.1), and that this trend is statistically significant to the 99.9 percentile confidence intervals.

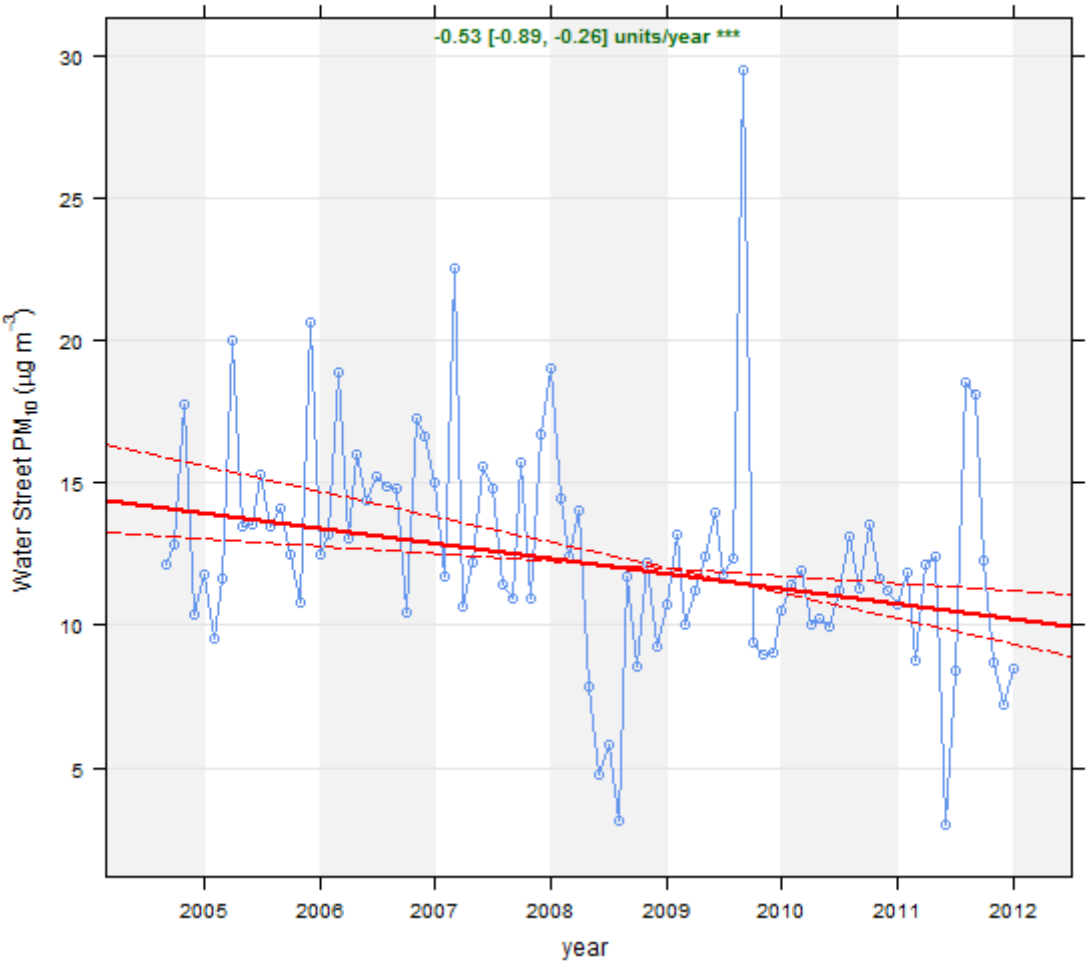

Figure 5.1 Trend analysis (deseasonalised) for PM_{10} at the Water Street site. The solid red line indicates the trend estimate, while the dashed red lines indicate the 95% confidence intervals for the trend based on data resampling methods.

Strongly seasonal cycles for PM_{10} concentrations can affect the results of the trend analysis because it is not only the quantity and rate of emissions that dictate ambient concentrations, but meteorology and longer-term climate can also have significant influences on local pollutant concentrations (Trompetter et al., 2010). Therefore the data presented in Figure 5.1 were deseasonalised using the functionality in the openair statistical package. When the trends in PM_{10} concentrations were examined on a seasonal basis it was found that the long-term decrease in PM was most significant during autumn and winter (95% CL) as shown in Figure 5.2.

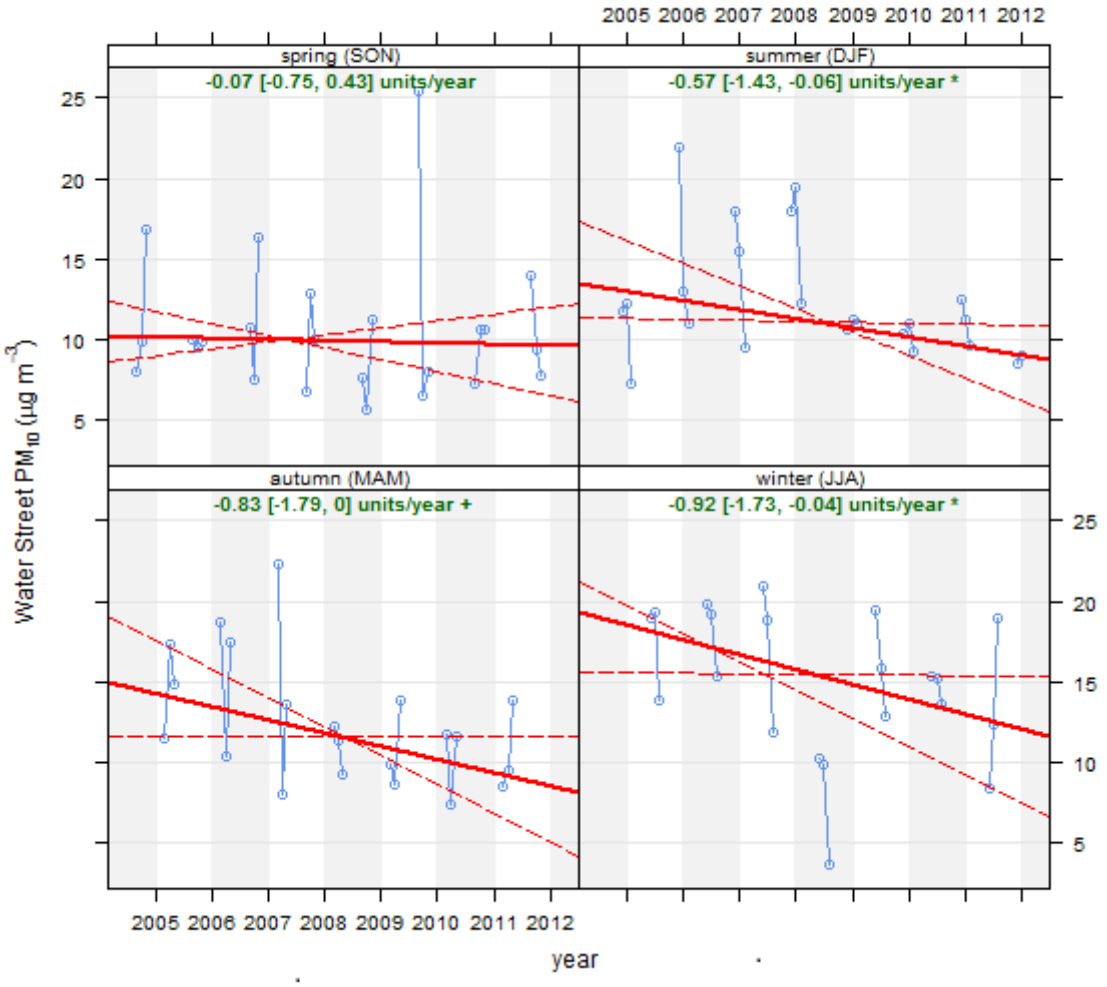

Figure 5.2 Seasonal trend analysis for PM_{10} at the Water Street site. The solid red line indicates the trend estimate, while the dashed red lines indicate the 95% confidence intervals for the trend based on data resampling methods.

To explain the decrease in PM_{10} concentrations it is necessary to examine the trends in source contributions. Firstly the total combustion source contributions were examined by analysing the black carbon data as discussed in Section 5.2.

5.2 TRENDS IN BLACK CARBON CONCENTRATIONS

The BC dataset provides the opportunity to examine the relative influence of combustion sources on PM_{10} over the same time period, since BC is primarily produced by combustion processes (biomass burning, motor vehicles and industrial installations). The relationship between PM_{10} and BC is strong because peak PM_{10} concentrations in the Whangarei airshed are driven by local combustion source activity (emissions from motor vehicles and biomass burning), as shown by the scatterplot presented in Figure 5.3. The exception to this is the PM_{10} sample with the concentration at 70 µg m^{-3} which has been identified as primarily composed of crustal matter.

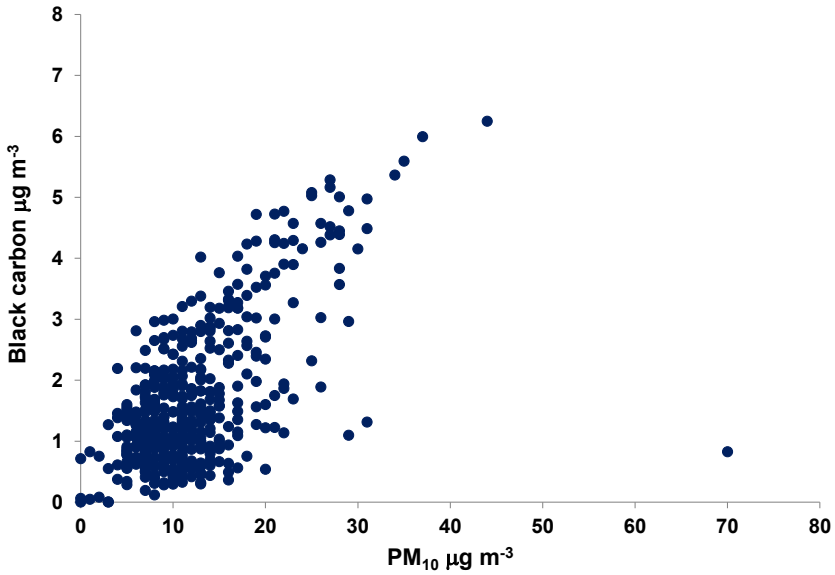

Figure 5.3 Scatterplot of black carbon concentrations (ng m^{-3}) versus PM_{10} concentrations (µg m^{-3}) at Water Street.

The analysis of trends in the BC concentration data (2004–2012) shows that year-on-year BC concentrations are decreasing (Figure 5.4), and that this trend is statistically significant to the 99.9 percentile confidence intervals.

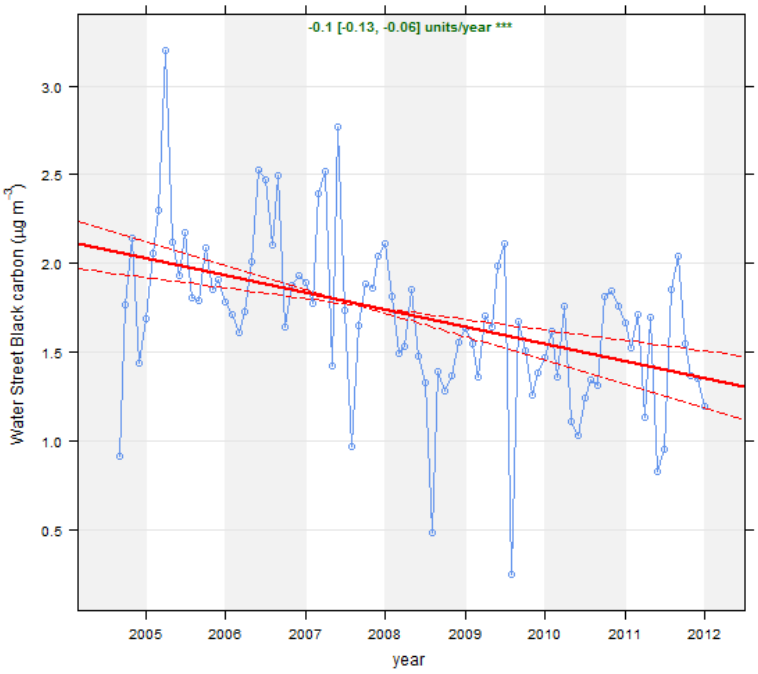

Figure 5.4 Trend analysis (deseasonalised) for Black Carbon concentrations at the Water Street site. The solid red line indicates the trend estimate, while the dashed red lines indicate the 95% confidence intervals for the trend based on data resampling methods.

Figure 5.4 shows that BC decreasing at 0.1 µg m^{-3} per year (99.9% confidence interval). The trends in BC concentrations on a seasonal basis it was found that the long-term decrease in BC was most significant during winter (99% CL) as shown in Figure 5.5.

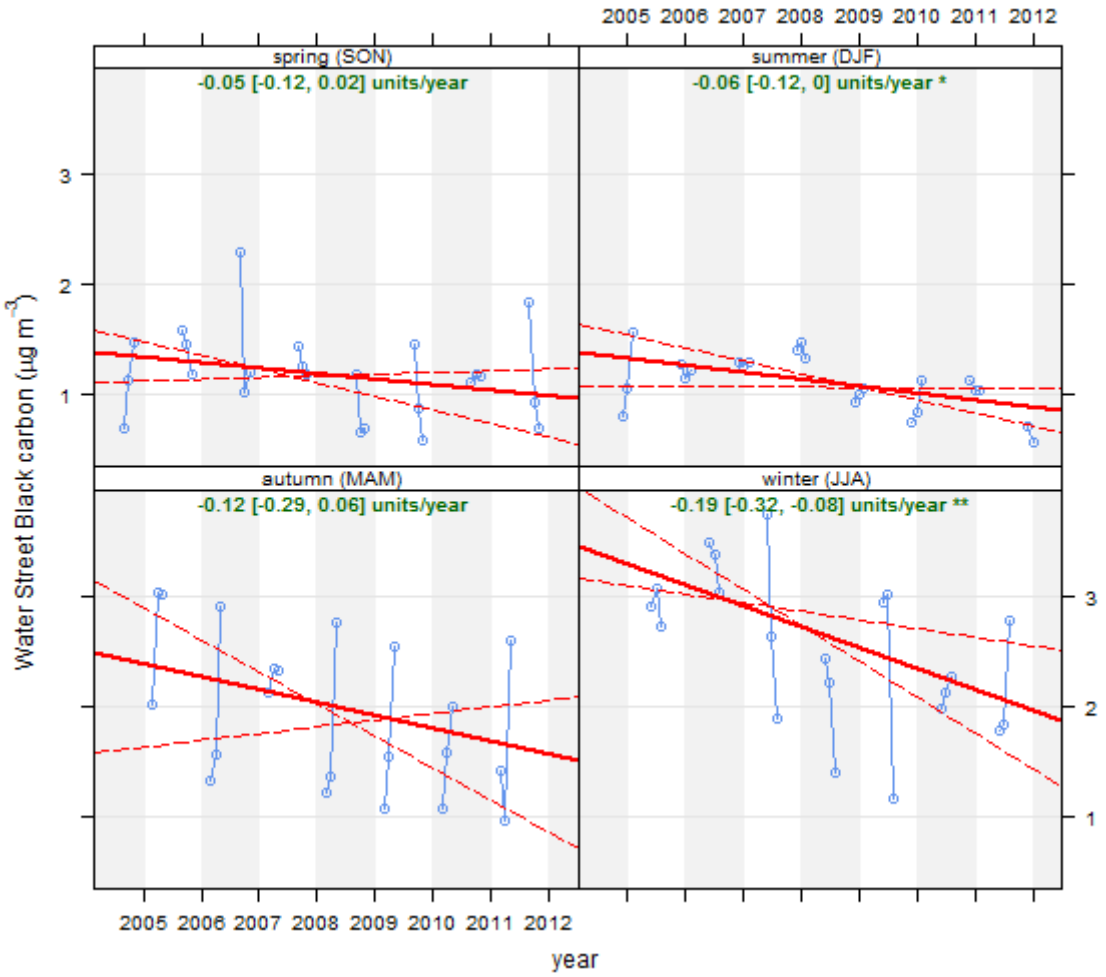

Figure 5.5 Seasonal trend analysis for Black Carbon concentrations at the Water Street site. The solid red lines indicate the trend estimates, while the dashed red lines indicate the 95% confidence intervals based on data resampling methods.

Interestingly, the data suggests that there has also been a significant (95% confidence interval) decrease in summer BC concentrations and this may reflect the introduction of outdoor burning restrictions in the Whangarei airshed and further afield.

The data shows that both PM_{10} and BC concentrations have been decreasing over the years 2004–2012, indicating that it was most likely to be a reduction in combustion source emissions affecting PM_{10} concentrations with the most significant reductions occurring during winter months.

5.3 TRENDS IN COMBUSTION SOURCE CONTRIBUTIONS TO PM_{10}

The receptor modelling analyses for PM_{10} sources presented in Chapter 4, found that biomass combustion and motor vehicle emissions were the primary sources of combustion related particulate matter in the Whangarei airshed and are therefore the major anthropogenic emission sources. The receptor modelling data was recompiled to provide source contributions to BC rather than PM_{10} because of the contribution of coarse particle road dust and wind-blown crustal matter to motor vehicle related particulate matter concentrations. While BC concentrations related to biomass combustion or motor vehicle emissions may change with a reduction in domestic fire use or improved engine emissions respectively, the road dust component is likely to behave independently (depending on road

type, traffic density, etc.) and therefore confound any trend analysis. When the trend analysis was applied to the source apportionment data for motor vehicle and biomass combustion source contributions to BC, it was found that the reduction in biomass combustion-related BC was primarily responsible for the BC reductions (99.9% confidence interval) as shown in Figure 5.6. The analysis did not indicate that there was any statistically significant trend in motor vehicle-related BC.

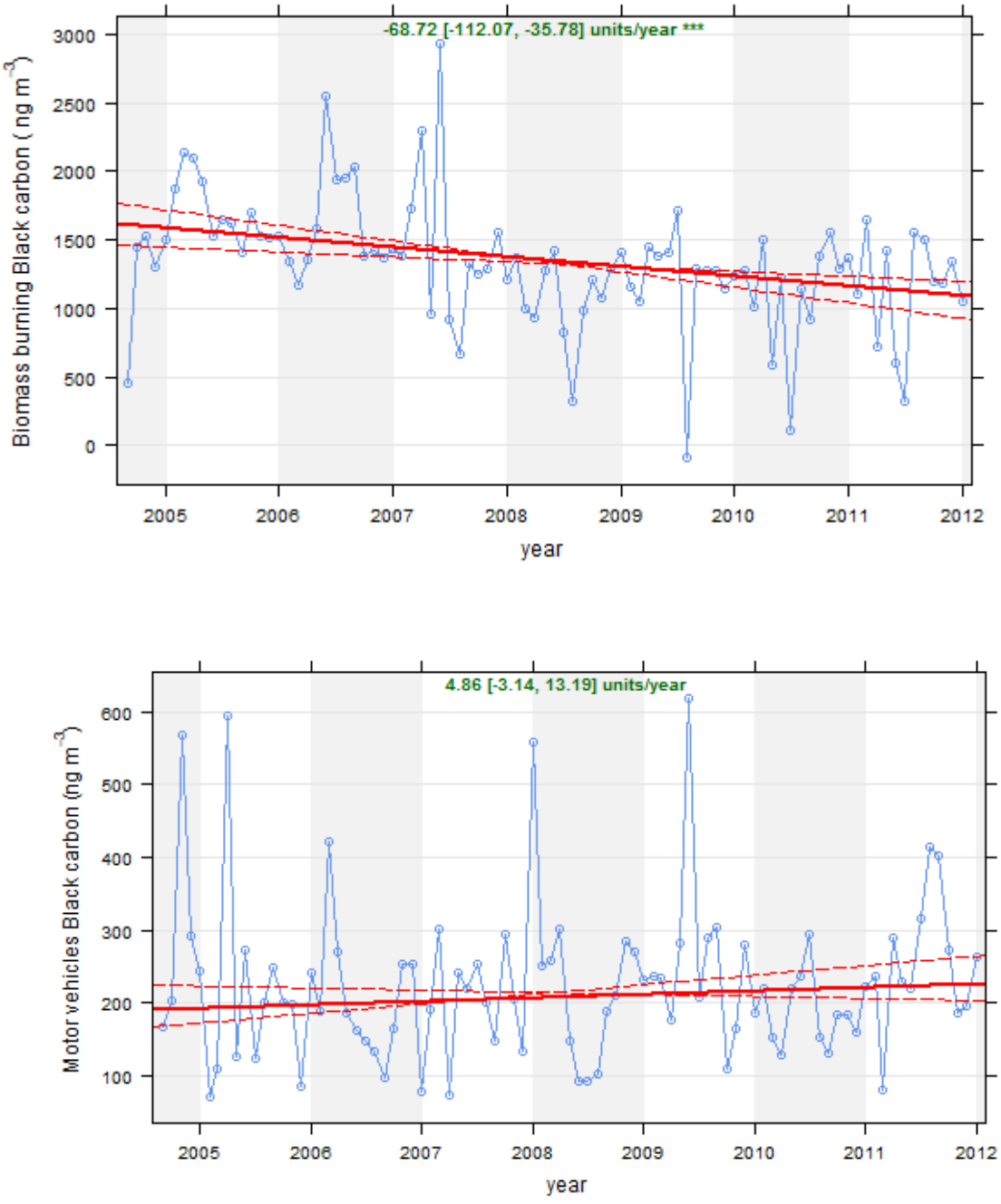

Figure 5.6 Trend analysis (deseasonalised) for biomass combustion (Top) and motor vehicle-related (Bottom) black carbon concentrations at the Water Street site. The solid red lines indicate the trend estimates, while the dashed red lines indicate the 95% confidence intervals based on data resampling methods.

When the trends in BC concentrations were examined on a seasonal basis, the data shows that the biomass burning was the major winter source and that emissions are decreasing. However, motor vehicle-related BC was found to actually be increasing during winter (95% confidence interval) and could reflect a growth in traffic and/or an increase in the diesel powered fleet since most particulate matter black carbon emissions from the motor vehicle fleet are primarily produced by diesel-powered engines.

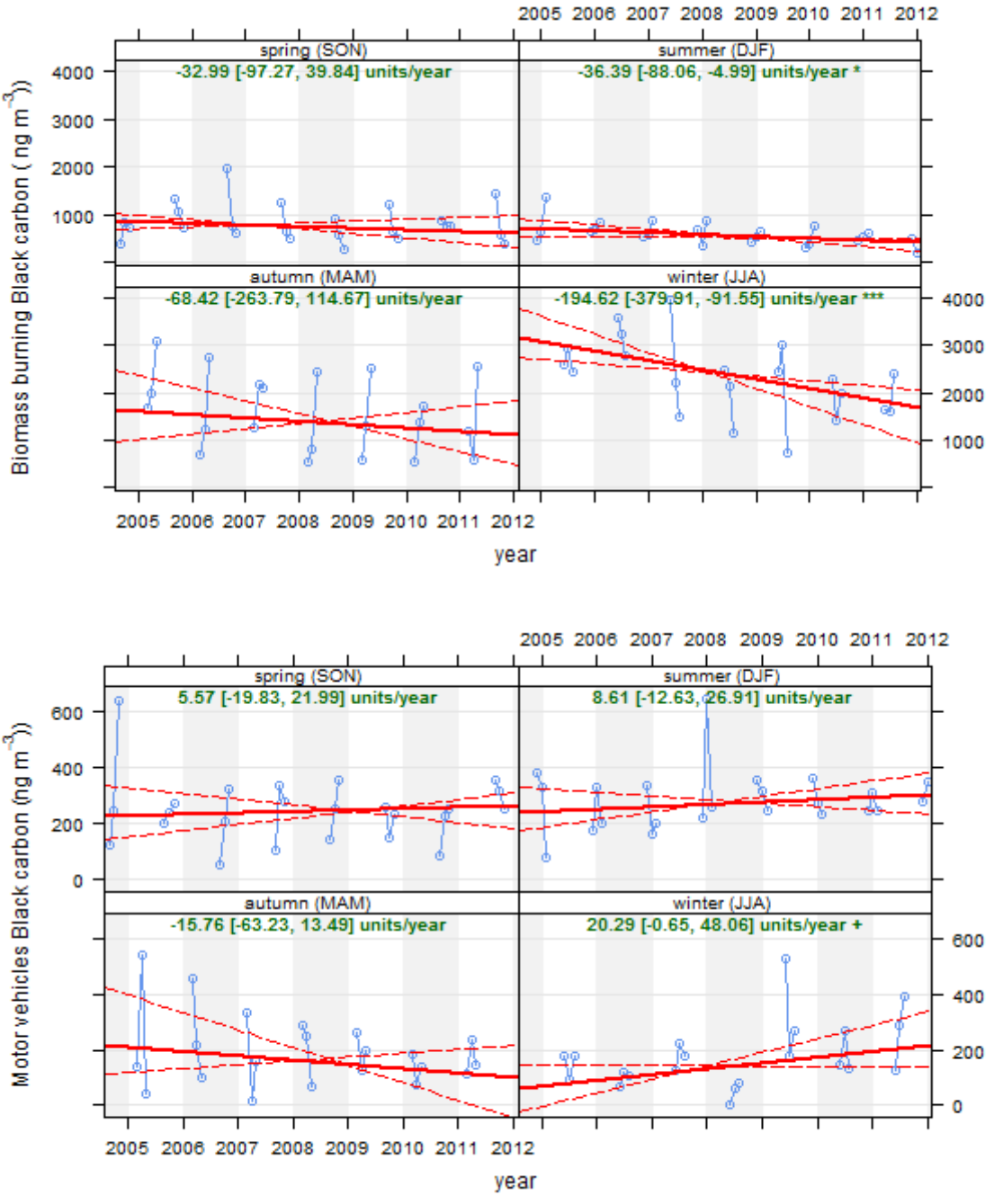

Figure 5.7 Seasonal trend analysis for biomass combustion (Top) and motor vehicle-related (Bottom) black carbon concentrations at the Water Street site. The solid red lines indicate the trend estimates, while the dashed red lines indicate the 95% confidence intervals based on data resampling methods.

5.4 TRENDS IN ARSENIC AND LEAD CONCENTRATIONS

The receptor modelling results for PM_{10} samples collected (2004–2012) at the Water Street site (Chapter 4) have shown that arsenic and lead were strongly associated with the biomass burning source. This was related of the use of copper chrome arsenate (CCA)-treated timber and timber that has been painted with lead containing paints as part of the fuel stream in domestic fires. The data here, and from other studies in New Zealand (Davy et al., 2012, Davy et al., 2011), indicate that the As is confined to the $PM_{2.5}$ size fraction and so too will be the lead contamination.

The XRF elemental data for lead and arsenic were examined for any significant trends in ambient concentrations. However, as presented in Figures 5.8 and 5.9, there was no statistically significant trend observed for arsenic and lead concentrations.

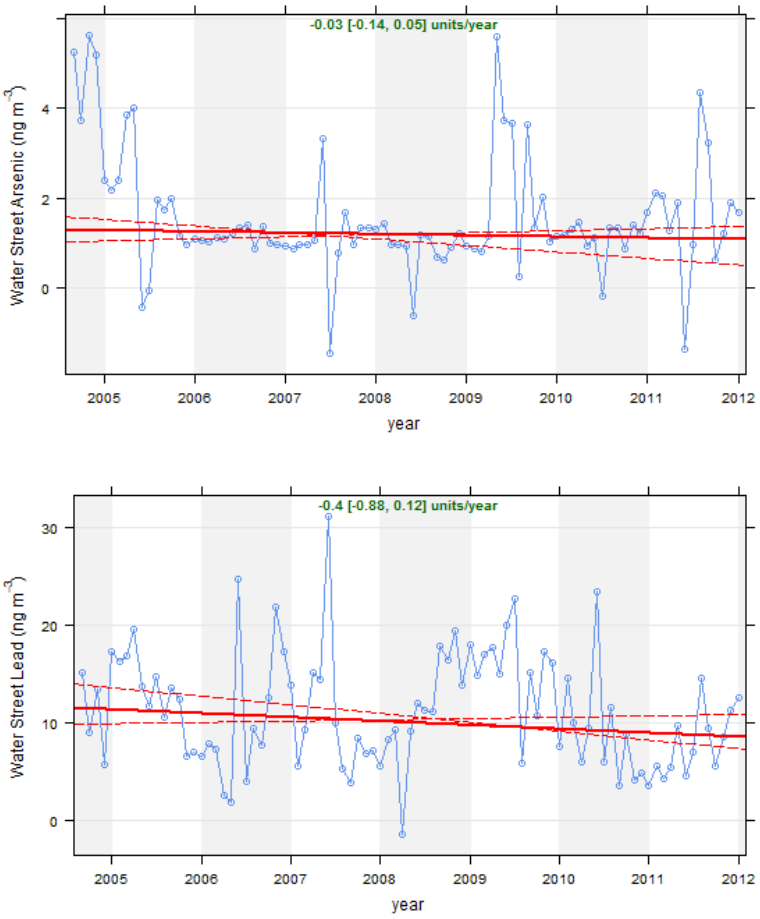

Figure 5.8 Trend analysis (deseasonalised) for arsenic (Top) and lead (Bottom) elemental concentrations at the Water Street site. The solid red lines indicate the trend estimates, while the dashed red lines indicate the 95% confidence intervals based on data resampling methods.

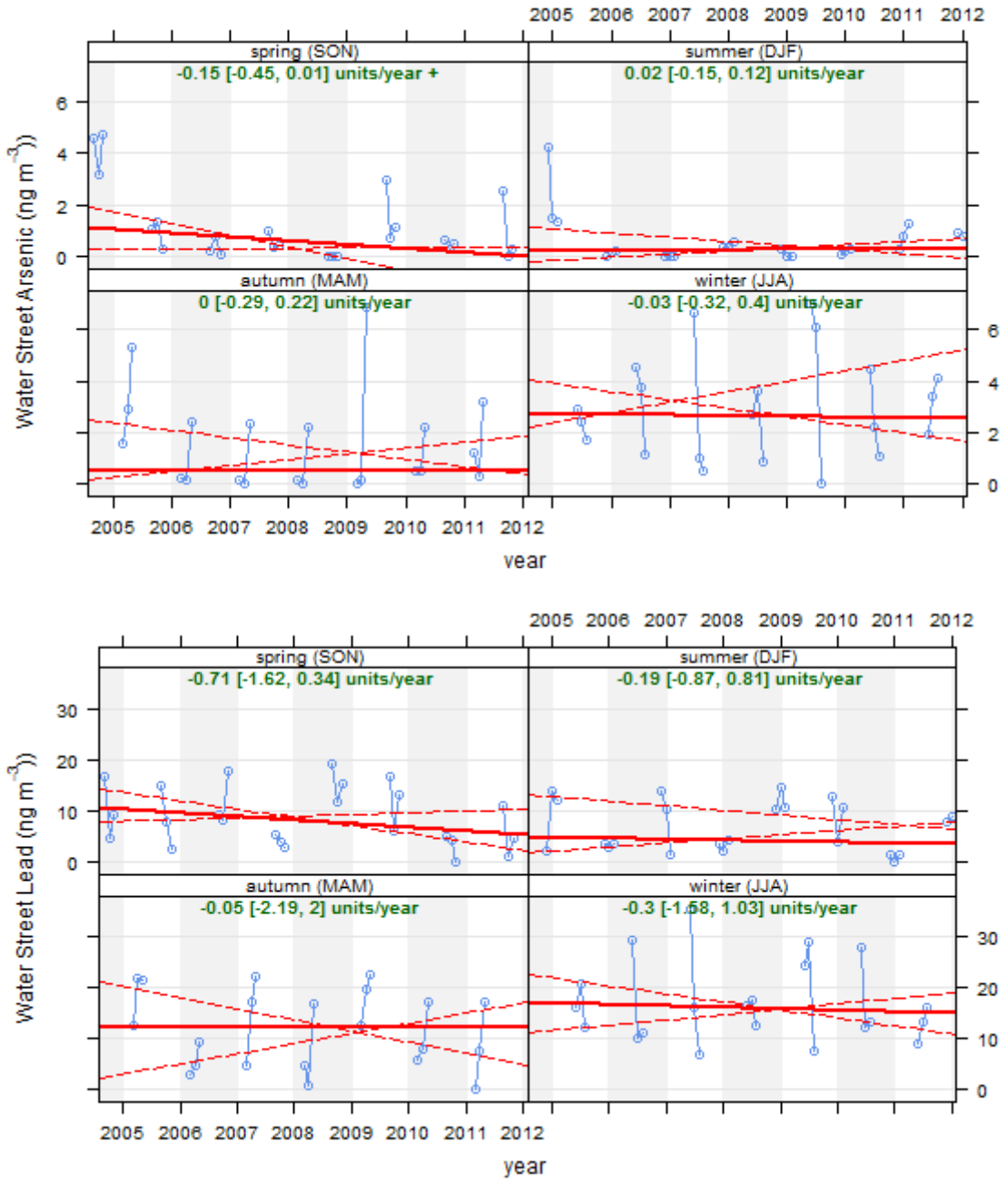

Figure 5.9 Seasonal trend analysis for arsenic (Top) and lead (Bottom) elemental concentrations at the Water Street site. The solid red lines indicate the trend estimates, while the dashed red lines indicate the 95% confidence intervals based on data resampling methods.

The reason for the lack in any statistically significant trend in arsenic or lead concentrations despite the observed decrease in biomass burning related particulate matter concentrations is somewhat uncertain. It suggests that similar amounts (on average) of the contaminants are being emitted each year. Alternatively there may be sufficient analytical noise in the data to confound any trend analysis. Further work would need to be done to establish the reasons for the discrepancy.

This page is intentionally left blank.

6.0 SUMMARY OF WATER STREET PM_{10} COMPOSITIONAL ANALYSIS

The elemental analysis and source apportionment of PM_{10} samples from the Water Street air quality monitoring site in Whangarei has provided a wealth of information and key findings have been summarised in the following sections.

6.1 COMPOSITION OF PM_{10}

Elemental and black carbon (BC) concentrations in PM_{10} samples were determined using X-ray fluorescence (XRF) and light reflection respectively. The PM_{10} samples from the Water Street site were collected on glass fibre filter material which is composed primarily of silicon dioxide along with alkali earth metals (Na, Mg, Ca, K). The XRF analysis showed that Na, Mg, K, Al, Si and Ca concentrations in particulate matter could not be determined accurately because they were either part of the composition of the filter matrix, or were present as impurities. For many other elements though, particularly those with atomic numbers equal or higher than titanium, sensible concentration data was able to be extracted. It was found that BC was an important component of PM_{10} as an indicator of combustion source emissions. Chlorine and sulphur had the second and third highest average concentrations respectively. Arsenic and lead were found to be present in PM_{10} samples at concentrations above their limits of detection and the time series for both elements showed winter peaks in concentrations.

6.2 SOURCES OF PM_{10}

Four sources were extracted from the PM_{10} elemental composition data by receptor modelling techniques to identify the primary contributing sources to PM_{10} in the Whangarei airshed. The four sources were identified to be a mixed motor vehicle and crustal matter source (38%), marine aerosol (seasalt) (26%), biomass burning (wood fires for home heating) (15%) and secondary sulphate (7%). Of the average PM_{10} mass (12 µg m^{-3}), 2.1 ± 1.0 µg m^{-3} was not attributed to any particular source. As concentration data for all major elemental components (e.g., Na, Mg, Al, Si, Ca, K) of particulate matter was not able to be extracted due to the filter matrix effects there was some uncertainty in the absolute mass contributions from each source type and the results should be considered indicative only.

6.2.1 Temporal patterns in source contributions

The source chemical profiles and the temporal variations in the PM_{10} source contributions were considered to be strongly representative of the identified sources. It was evident that PM_{10} mass was dominated by the biomass combustion source during winter, which arises primarily from solid fuel (wood burning) fire emissions used for domestic heating. During other time periods, motor vehicles, crustal matter and marine aerosol were the primary sources of particulate matter at the Water Street site. Both arsenic and lead were strongly associated with the biomass combustion source and this was considered to be through the use of copper chrome arsenate treated timber and timber that had been painted with lead containing paints as fuel in domestic fires.

6.3 TRENDS IN PM_{10} CONCENTRATIONS AND SOURCE CONTRIBUTIONS

The data were examined for temporal trends and it was found that both PM_{10} and black carbon concentrations were decreasing over the 7-year monitoring period. When the black carbon data were broken down by combustion source contributions it was found the there was a decreasing trend in biomass burning (and by inference a reduction in domestic fire emissions) and that this was driving the reduction in PM_{10} concentrations. No significant trend was evident for the motor vehicle combustion source. Additionally when temporal patterns for arsenic and lead were analysed there did not appear to be any statistically significant trend in concentrations for these elements despite the linkage to domestic fire emissions. The reason for this may lie with analytical uncertainty in the elemental data but is indeterminate at this stage.

6.4 IMPLICATIONS FOR AIR QUALITY MANAGEMENT

Overall the trending reduction in PM_{10} concentrations due to decreasing domestic fire emissions is a positive outcome for air quality management in the Whangarei airshed and the associated human health implications from exposure to this source. However, the presence of arsenic and lead in PM_{10} associated with domestic fire emissions raises questions as to why fuels contaminated with these elements are finding their way into the fuel supply. This is particularly relevant since use of such contaminated fuel is banned by the Regional Air Plan.

Moreover, the Water Street monitoring site was located in the CBD area of Whangarei City and was therefore somewhat removed from the residential locations where emissions were likely to occur. Consequently the measured elemental concentrations for species such as arsenic and lead at Water Street would be less than in a residential area and therefore the true exposure to these contaminants may be higher. Consideration must also be given to indoor air quality in the houses of those residents who use such contaminated fuels and the potential for adverse health effects on the inhabitants.

6.5 RECOMMENDATIONS

Given the presence of arsenic and lead contamination in PM_{10} and the link to domestic wood fires, Northland Regional Council may wish to consider monitoring campaigns to investigate the extent of the problem with a particular focus on residential locations where exposure is likely to be highest (i.e., neighbourhoods with a high percentage of domestic solid fuel fires).

7.0 REFERENCES

ANCELET, T., DAVY, P. K., MITCHELL, T., TROMPETTER, W. J., MARKWITZ, A. & WEATHERBURN, D. C. 2012. Identification of particulate matter sources on an hourly time-scale in a wood burning community. *Environmental Science and Technology,* 46**,** 4767-4774.

BEGUM, B. A., HOPKE, P. K. & ZHAO, W. X. 2005. Source identification of fine particles in Washington, DC, by expanded factor analysis modeling. *Environ. Sci. Technol.,* 39**,** 1129-1137.

BROWN, S. G. & HAFNER, H. R. 2005. Multivariate Receptor Modelling Workbook. Research Triangle Park, NC: USEPA.

CAHILL, T. A., ELDRED, R. A., MOTALLEBI, N. & MALM, W. C. 1989. Indirect measurement of hydrocarbon aerosols across the United States by nonsulfate hydrogen-remaining gravimetric mass correlations. *Aerosol Sci. Technol.,* 10**,** 421-9.

CARSLAW, D. C. 2012. The openair manual - open-source tools for analysing air pollution data. Manual for version 0.7-0. King's College London.

CARSLAW, D. C. & ROPKINS, K. 2012. openair - an R package for air quality data analysis. *Environmental Modelling & Software,* 27-28**,** 52-61.

CHUEINTA, W., HOPKE, P. K. & PAATERO, P. 2000. Investigation of sources of atmospheric aerosol at urban and suburban residential areas in Thailand by positive matrix factorization. *Atmos. Environ.,* 34**,** 3319-3329.

COHEN, D., TAHA, G., STELCER, E., GARTON, D. & BOX, G. The measurement and sources of fine particle elemental carbon at several key sites in NSW over the past eight years. 15th Clean Air Conference, 2000 Sydney. Clean air Society of Australia and New Zealand.

COHEN, D. D. 1999. Accelerator based ion beam techniques for trace element aerosol analysis. *Advances in Environmental, Industrial and Process Control Technologies,* 1**,** 139-196.

CRAW, D., CHAPPELL, D. & REAY, A. 2000. Environmental mercury and arsenic sources in fossil hydrothermal systems, Northland, New Zealand. *Environmental Geology,* 39**,** 875-887.

CRAW, D., FALCONER, D. & YOUNGSON, J. H. 2003. Environmental arsenopyrite stability and dissolution: Theory, experiment, and field observations. *Chemical Geology,* 199**,** 71-82.

DAVY, P., K. 2007. Composition and Sources of Aerosol in the Wellington Region of New Zealand. PhD Thesis. *School of Chemical and Physical Sciences.* Wellington: Victoria University of Wellington.

DAVY, P., K., TROMPETTER, W. & MARKWITZ, A. 2009a. Source apportionment of airborne particles at Wainuiomata, Lower Hutt. Wellington: GNS Science Client Report 2009/188.

DAVY, P., K., TROMPETTER, W. & MARKWITZ, A. 2009b. Source apportionment of airborne particles in the Auckland region: 2008 Update. Wellington: GNS Science Client Report 2009/165.

DAVY, P., K., TROMPETTER, W. J. & MARKWITZ, A. 2007. Source apportionment of airborne particles in the Auckland region. Wellington: GNS Science Client Report 2007/314.

DAVY, P., K., TROMPETTER, W. J. & MARKWITZ, A. 2008. Source apportionment of airborne particles at Seaview, Lower Hutt. Wellington: GNS Science Client Report 2008/160.

DAVY, P. K., ANCELET, T., TROMPETTER, W. J., MARKWITZ, A. & WEATHERBURN, D. C. 2012. Composition and source contributions of air particulate matter pollution in a New Zealand suburban town. *Atmospheric Pollution Research,* 3**,** 143-147.

DAVY, P. K., TROMPETTER, W. J. & MARKWITZ, A. 2011. Source apportionment of airborne particles in the Auckland region: 2010 Analysis. Wellington: GNS Science Client Report 2010/262.

EBERLY, S. 2005. EPA PMF 1.1 User's Guide. USEPA.

FINE, P. M., CASS, G. R. & SIMONEIT, B. R. 2001. Chemical characterization of fine particle emissions from fireplace combustion of woods grown in the northeastern United States. *Environ. Sci. Technol.,* 35**,** 2665-75.

FUNG, K., CHOW JUDITH, C. & WATSON JOHN, G. 2002. Evaluation of OC/EC speciation by thermal manganese dioxide oxidation and the IMPROVE method. *Journal of the Air & Waste Management Association (1995),* 52**,** 1333-41.

HELSEN, L. & VAN DEN BULCK, E. 2003. Metal Retention in the Solid Residue after Low-Temperature Pyrolysis of Chromated Copper Arsenate (CCA)-Treated Wood. *Environmental Engineering Science,* 20**,** 569-580.

HOPKE, P. K., XIE, Y. L. & PAATERO, P. 1999. Mixed multiway analysis of airborne particle composition data. *J. Chemomet.,* 13**,** 343-352.

HORVATH, H. 1993. Atmospheric Light Absorption - A Review. *Atmos. Environ,,* 27A**,** 293-317.

HORVATH, H. 1997. Experimental calibration for aerosol light absorbtion measurements using the integrating plate method - Summary of the data. *Aerosol Science,* 28**,** 2885-2887.

JACOBSON, M. C., HANSSON, H. C., NOONE, K. J. & CHARLSON, R. J. 2000. Organic atmospheric aerosols: review and state of the science. *Reviews of Geophysics,* 38**,** 267-294.

JEONG, C.-H., HOPKE, P. K., KIM, E. & LEE, D.-W. 2004. The comparison between thermal-optical transmittance elemental carbon and Aethalometer black carbon measured at multiple monitoring sites. *Atmos. Environ.,* 38**,** 5193.

KIM, E., HOPKE, P. K. & EDGERTON, E. S. 2003. Source identification of Atlanta aerosol by positive matrix factorization. *J. Air Waste Manage. Assoc.,* 53**,** 731-739.

KIM, E., HOPKE, P. K., LARSON, T. V., MAYKUT, N. N. & LEWTAS, J. 2004. Factor analysis of Seattle fine particles. *Aerosol Sci. Technol.,* 38**,** 724-738.

LEE, E., CHAN, C. K. & PAATERO, P. 1999. Application of positive matrix factorization in source apportionment of particulate pollutants in Hong Kong. *Atmos. Environ,,* 33**,** 3201-3212.

LEE, J. H., YOSHIDA, Y., TURPIN, B. J., HOPKE, P. K., POIROT, R. L., LIOY, P. J. & OXLEY, J. C. 2002. Identification of sources contributing to Mid-Atlantic regional aerosol. *J. Air Waste Manag. Assoc.,* 52**,** 1186-1205.

LI, X., GE, L., DONG, Y. & CHANG, H. C. Estimating the greatest dust storm in eastern Australia with MODIS satellite images. International Geoscience and Remote Sensing Symposium (IGARSS), 2010 Honolulu, HI. 1039-1042.

LIDE, D. R. 1992. *CRC Handbook of Chemistry and Physics*, CRC Press Inc.

LONGHURST, R. D., ROBERTS, A. H. C. & WALLER, J. E. 2004. Concentrations of arsenic, cadmium, copper, lead, and zinc in New Zealand pastoral topsoils and herbage. *New Zealand Journal of Agricultural Research,* 47**,** 23-32.

MALM, W. C., SISLER, J. F., HUFFMAN, D., ELDRED, R. A. & CAHILL, T. A. 1994. Spatial and seasonal trends in particle concentration and optical extinction in the United States. *J. Geophys. Res. Atmos.,* 99**,** 1347-70.

MFE 2002. New Zealand Ambient Air Quality Guidelines. Wellington: New Zealand Government.

PAATERO, P. 1997. Least squares formulation of robust non-negative factor analysis. *Chemom. Intell. Lab. Syst.,* 18**,** 183-194.

PAATERO, P. 2000. PMF User's Guide. Helsinki: University of Helsinki.

PAATERO, P. & HOPKE, P. K. 2002. Utilizing wind direction and wind speed as independent variables in multilinear receptor modeling studies. *Chemometrics and Intelligent Laboratory Systems,* 60**,** 25-41.

PAATERO, P. & HOPKE, P. K. 2003. Discarding or downweighting high-noise variables in factor analytic models. *Analytica Chimica Acta,* 490**,** 277-289.

PAATERO, P., HOPKE, P. K., BEGUM, B. A. & BISWAS, S. K. 2005. A graphical diagnostic method for assessing the rotation in factor analytical models of atmospheric pollution. *Atmospheric Environment,* 39**,** 193-201.

PAATERO, P., HOPKE, P. K., SONG, X. H. & RAMADAN, Z. 2002. Understanding and controlling rotations in factor analytic models. *Chemometrics and Intelligent Laboratory Systems,* 60**,** 253-264.

RAMADAN, Z., EICKHOUT, B., SONG, X.-H., BUYDENS, L. M. C. & HOPKE, P. K. 2003. Comparison of Positive Matrix Factorization and Multilinear Engine for the source apportionment of particulate pollutants. *Chemomet. Intellig. Lab. Syst.,* 66**,** 15-28.

ROBINSON, B., CLOTHIER, B., BOLAN, N., MAHIMAIRAJA, S., GREVEN, M., MONI, C., MARCHETTI, M., VAN DEN DIJSSEL, C. & MILNE, G. Arsenic in the New Zealand Environment. 3rd Australian New Zealand Soils Conference, 2004 Sydney, Australia.

SALMA, I., CHI, X. & MAENHAUT, W. 2004. Elemental and organic carbon in urban canyon and background environments in Budapest, Hungary. *Atmos. Environ.,* 38**,** 27-36.

SCOTT, A. J. 2006. *Source Apportionment and Chemical Characterisation of Airborne Fine Particulate Matter in Christchurch, New Zealand.* PhD Thesis, University of Canterbury.

SHAH, P., STREZOV, V., STEVANOV, C. & NELSON, P. F. 2006. Speciation of Arsenic and Selenium in Coal Combustion Productsâ€ *Energy & Fuels,* 21**,** 506-512.

SIMMONS, S. F. & BROWNE, P. R. L. 2000. Hydrothermal minerals and precious metals in the Broadlands-Ohaaki geothermal system: Implications for understanding low-sulfidation epithermal environments. *Economic Geology,* 95**,** 971-999.

SONG, X. H., POLISSAR, A. V. & HOPKE, P. K. 2001. Sources of fine particle composition in the northeastern US. *Atmospheric Environment,* 35**,** 5277-5286.

TEAM, R. D. C. 2011. R: A language and environment for statistical computing. R Foundation for Statistical Computing, Vienna, Austria.

TROMPETTER, W. J. 2004. Ion Beam Analysis results of air particulate filters from the Wellington Regional Council. Wellington: Geological and Nuclear Sciences Limited.

TROMPETTER, W. J., DAVY, P. K. & MARKWITZ, A. 2010. Influence of environmental conditions on carbonaceous particle concentrations within New Zealand. *Journal of Aerosol Science,* 41**,** 134-142.

WATSON, J. G., ZHU, T., CHOW, J. C., ENGELBRECHT, J., FUJITA, E. M. & WILSON, W. E. 2002. Receptor modeling application framework for particle source apportionment. *Chemosphere,* 49**,** 1093-1136.

APPENDICES

This page is intentionally left blank.

APPENDIX 1: X-RAY FLUORESCENCE SPECTROSCOPY

X-ray fluorescence spectroscopy (XRF) was used to measure elemental concentrations in PM_{10} samples collected on glass fibre filters at the Water Street monitoring site in Whangarei. XRF measurements in this study were carried out at the GNS Science XRF facility and the spectrometer used was a PANalytical Epsilon 5 (PANalytical, the Netherlands). The Epsilon 5 is shown in Figure A1.1. XRF is a non-destructive and relatively rapid method for the elemental analysis of particulate matter samples.

Figure A1.1 The PANalytical Epsilon 5 spectrometer.

XRF is based on the measurement of characteristic X-rays produced by the ejection of an inner shell electron from an atom in the sample, creating a vacancy in the inner atomic shell. A higher energy electron then drops into the lower energy orbital and releases a fluorescent X-ray to remove excess energy (Watson et al., 1999 and references therein). The energy of the released X-ray is characteristic of the emitting element and the area of the fluorescent X-ray peak (intensity of the peak) is proportional to the number of emitting atoms in the sample. From the intensity it is possible to calculate a specific element's concentration by direct comparison with standards.

To eject inner shell electrons from atoms in a sample, XRF spectrometer at GNS Science uses a 100 kV Sc/W X-ray tube. The 100 kV X-rays produced by this tube are able to provide elemental information for elements from Na–U. Unlike ion beam analysis techniques, which are similar to XRF, the PANalytical Epsilon 5 is able to use characteristic K-lines produced by each element for quantification. This is crucial for optimising limits of detection because K-

lines have higher intensities and are located in less crowded regions of the X-ray spectrum. The X-rays emitted by the sample are detected using a high performance Ge detector, which further improves the detection limits. Figure A1.2 presents a sample X-ray spectrum of the Water Street samples.

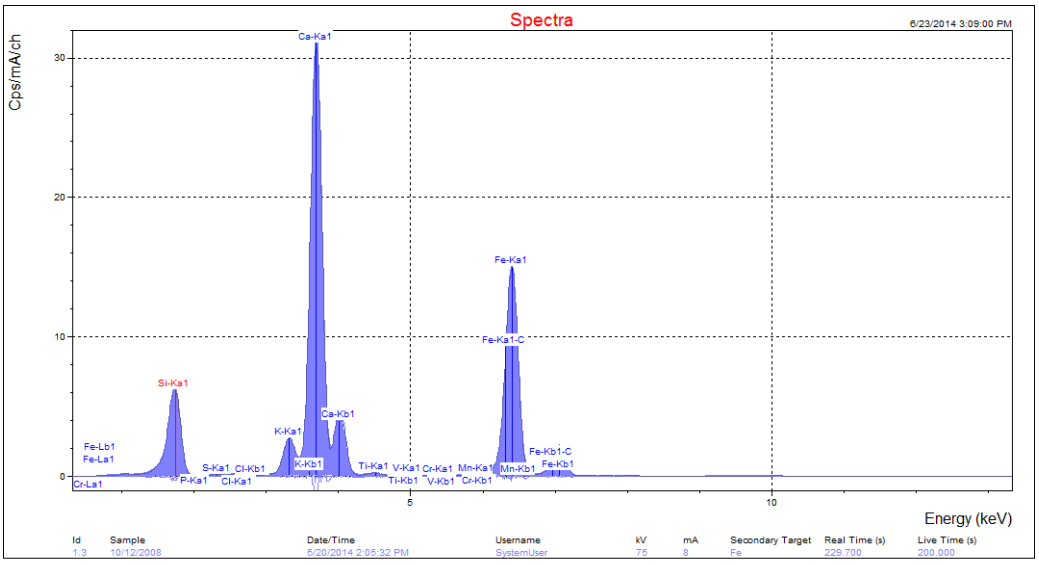

Figure A1.2 Example X-ray spectrum from a PM_{10} sample collected at Water Street.

In this study, calibration standards for each of the elements of interest were analysed prior to the samples being run. Once the calibration standards were analysed, spectral deconvolutions were performed using PANalytical software to correct for line overlaps and ensure that the spectra were accurately fit. Calibration curves for each element of interest were produced and used to determine the elemental concentrations from the Water Street samples. A NIST reference sample was also analysed to ensure that the results obtained were robust and accurate.

References

Watson, J. G., Chow, J. C., Frazier, C. A., 1999. X-ray Fluorescence Analysis of Ambient Air Samples, in *Advances in Environmental, Industrial and Process Control Technologies* 1, 139–196.

A1.1 BLACK CARBON MEASUREMENTS

Black carbon (BC) has been studied extensively, but it is still not clear to what degree it is elemental carbon (EC (or graphitic) C(0)) or high molecular weight refractory weight organic species or a combination of both (Jacobson et al., 2000). Current literature suggests that BC is likely a combination of both, and that for combustion sources such as petrol and diesel fuelled vehicles and biomass combustion (wood burning, coal burning), EC and organic carbon compounds (OC) are the principle aerosol components emitted (Fine et al., 2001, Jacobson et al., 2000, Salma et al., 2004, Watson et al., 2002).

Determination of carbon (soot) on filters was performed by light reflection to provide the BC concentration. The absorption and reflection of visible light on particles in the atmosphere or collected on filters is dependent on the particle concentration, density, refractive index and size. For atmospheric particles, BC is the most highly absorbing component in the visible

light spectrum with very much smaller components coming from soils, sulphates and nitrate (Horvath, 1993, Horvath, 1997). Hence, to the first order it can be assumed that all the absorption on atmospheric filters is due to BC. The main sources of atmospheric BC are anthropogenic combustion sources and include biomass burning, motor vehicles and industrial emissions (Cohen et al., 2000). Cohen and co-workers found that BC is typically 10–40% of the fine mass ($PM_{2.5}$) fraction in many urban areas of Australia.

When measuring BC by light reflection/transmission, light from a light source is transmitted through a filter onto a photocell. The amount of light absorption is proportional to the amount of black carbon present and provides a value that is a measure of the black carbon on the filter. Conversion of the absorbance value to an atmospheric concentration value of BC requires the use of an empirically derived equation (Cohen et al., 2000):

$$BC\ (\mu g\ cm^{-2}) = (100/2(F\varepsilon))\ \ln[R_0/R] \qquad \textbf{(A1.2)}$$

where:

ε is the mass absorbent coefficient for BC ($m^2\ g^{-1}$) at a given wavelength;

F is a correction factor to account for other absorbing factors such as sulphates, nitrates, shadowing and filter loading. These effects are generally assumed to be negligible and F is set at 1.00;

R_0, R are the pre- and post-reflection intensity measurements, respectively.

Black carbon was measured at GNS Science using the M43D Digital Smoke Stain Reflectometer. The following equation (from Willy Maenhaut, Institute for Nuclear Sciences, University of Gent Proeftuinstraat 86, B-9000 GENT, Belgium) was used for obtaining BC from reflectance measurements on Nucleopore polycarbonate filters or Pall Life Sciences Teflon filters:

$$BC\ (\mu g\ cm^{-2}) = [1000 \times LOG(R_{blank}/R_{sample}) + 2.39] / 45.8 \qquad \textbf{(A1.3)}$$

where:

R_{blank}: the average reflectance for a series of blank filters; R_{blank} is close (but not identical) to 100. GNS always use the same blank filter for adjusting to 100.

R_{sample}: the reflectance for a filter sample (normally lower than 100).

With: 2.39 and 45.8 constants derived using a series of 100 Nuclepore polycarbonate filter samples which served as secondary standards; the BC loading (in $\mu g\ cm^{-2}$) for these samples had been determined by Prof. Dr. M.O. Andreae (Max Planck Institute of Chemistry, Mainz, Germany) relative to standards that were prepared by collecting burning acetylene soot on filters and determining the mass concentration gravimetrically (Trompetter, 2004).

APPENDIX 2: POSITIVE MATRIX FACTORISATION

Positive matrix factorisation (PMF) is a linear least-squares approach to factor analysis and was designed to overcome the receptor modeling problems associated with techniques like principal components analysis (PCA) (Paatero et al., 2005). With PMF, sources are constrained to have non-negative species concentrations, no sample can have a negative source contribution and error estimates for each observed data point are used as point-by-point weights. This feature is a distinct advantage, in that it can accommodate missing and below detection limit data that is a common feature of environmental monitoring results (Song et al., 2001). In fact, the signal to noise ratio for an individual elemental measurement can have a significant influence on a receptor model and modeling results. For the weakest (closest to detection limit) species, the variance may be entirely from noise (Paatero and Hopke, 2002). Paatero and Hopke strongly suggest down-weighting or discarding noisy variables that are always below their detection limit or species that have a lot of error in their measurements relative to the magnitude of their concentrations (Paatero and Hopke, 2003). The distinct advantage of PMF is that mass concentrations can be included in the model and the results are directly interpretable as mass contributions from each factor (source).

A2.1 PMF MODEL OUTLINE

The mathematical basis for PMF is described in detail by Paatero (Paatero, 1997, Paatero, 2000). Briefly, PMF uses a weighted least-squares fit with the known error estimates of measured elemental concentrations used to derive the weights. In matrix notation this is indicated as:

$$X = GF + E \quad \textbf{(A2.1)}$$

where:

X is the known *n* x *m* matrix of *m* measured elemental species in *n* samples;

G is an *n* x *p* matrix of source contributions to the samples;

F is a *p* x *m* matrix of source compositions (source profiles).

E is a residual matrix – the difference between measurement *X* and model *Y.*

E can be defined as a function of factors *G* and *F*:

$$e_{ij} = x_{ij} - y_{ij} = x_{ij} - \sum_{k=1}^{p} g_{ik} f_{kj} \quad \textbf{(A2.2)}$$

where:

i = 1,……,*n* elements

j = 1,……,*m* samples

k = 1,…...,*p* sources

PMF constrains all elements of *G* and *F* to be non-negative, meaning that elements cannot have negative concentrations and samples cannot have negative source contributions as in real space. The task of PMF is to minimise the function *Q* such that:

$$Q(E) = \sum_{i=1}^{n} \sum_{j=1}^{m} (e_{ik} / \sigma_{kj})^2 \qquad \textbf{(A2.3)}$$

where σ_{ij} is the error estimate for x_{ij}. Another advantage of PMF is the ability to handle extreme values typical of air pollutant concentrations as well as true outliers that would normally skew PCA. In either case, such high values would have significant influence on the solution (commonly referred to as leverage). PMF has been successfully applied to receptor modeling studies in a number of countries around the world (Begum et al., 2005, Kim et al., 2004, Jeong et al., 2004, Kim et al., 2003, Lee et al., 2002, Song et al., 2001, Chueinta et al., 2000, Hopke et al., 1999, Lee et al., 1999) including New Zealand (Davy, 2007, Davy et al., 2009b, Davy et al., 2009a, Davy et al., 2007, Davy et al., 2008, Scott, 2006, Ancelet et al., 2012).

A2.2 PMF MODEL USED

Two programs have been written to implement different algorithms for solving the least squares PMF problem, these are PMF2 and EPAPMF, which incorporates the Multilinear Engine (ME-2) (Ramadan et al., 2003, Hopke et al., 1999). In effect, the EPAPMF program provides a more flexible framework than PMF2 for controlling the solutions of the factor analysis with the ability of imposing explicit external constraints.

This study used EPAPMF 5.0 (Version 5.1), a newly released software version which incorporates a graphical user interface (GUI) based on the ME-2 program along with multiple diagnostic routines to ensure a robust solution is obtained. Both PMF2 and EPAPMF programs can be operated in a robust mode, meaning that “outliers” are not allowed to overly influence the fitting of the contributions and profiles (Eberly, 2005). The user specifies two input files, one file with the concentrations and one with the uncertainties associated with those concentrations. The methodology for developing an uncertainty matrix associated with the elemental concentrations for this work is discussed in Section A2.4.2.

A2.3 PMF MODEL INPUTS

The PMF programs provide the user with a number of choices in model parameters that can influence the final solution. Two parameters, the 'signal-to-noise ratio' and the 'species category' are of particular importance and are described below.

Signal-to-noise ratio – this is a useful diagnostic statistic estimated from the input data and uncertainty files using the following calculation:

$$(1/2)\sqrt{\sum_{i=1}^{n}(x_{ij})^2 \Big/ \sum_{i=1}^{n}(\sigma_{ij})^2} \qquad \textbf{(A2.4)}$$

Where x_{ij} and σ_{ij} are the concentration and uncertainty, respectively, of the i^{th} element in the j^{th} sample. Smaller signal-to-noise ratios indicate that the measured elemental concentrations are generally near the detection limit and the user should consider whether to include that species in the receptor model or at least strongly down-weight it (Paatero and Hopke, 2003). The signal-to-noise ratios (S/N ratio) for each element are reported alongside other statistical data in the results section.

Species category – this enables the user to specify whether the elemental species should be considered:

- Strong – whereby the element is generally present in concentrations well above the LOD (high signal to noise ratio) and the uncertainty matrix is a reasonable representation of the errors.
- Weak – where the element may be present in concentrations near the LOD (low signal to noise ratio); there is doubt about some of the measurements and/or the error estimates; or the elemental species is only detected some of the time. If 'Weak' is chosen EPA.PMF increases the user-provided uncertainties for that variable by a factor of 3.
- Bad – that variable is excluded from the model run.

For this work, an element with concentrations at least 3 times above the LOD, a high signal to noise ratio (> 2) and present in all samples was considered 'Strong'. Variables were labelled as weak if their concentrations were generally low, had a low signal to noise ratio, were only present in a few samples or there was a lower level of confidence in their measurement. Mass concentration gravimetric measurements and BC were also down weighted as 'Weak' because their concentrations are generally several orders of magnitude above other species, which can have the tendency to 'pull' the model. Paatero and Hopke recommend that such variables be down weighted and that it doesn't particularly affect the model fitting if those variables are from real sources (Paatero and Hopke, 2003). What does affect the model severely is if a dubious variable is over-weighted. Elements that had a low signal to noise ratio (< 0.2), or had mostly missing (zero) values, or were doubtful for any reason, were labelled as 'Bad' and were subsequently not included in the analyses.

If the model is appropriate for the data and if the uncertainties specified are truly reflective of the uncertainties in the data, then *Q* (according to Eberly) should be approximately equal to the number of data points in the concentration data set (Eberly, 2005):

*Theoretical Q = # samples **x** # species measured* **(A2.5)**

However, a slightly different approach to calculating the Theoretical *Q* value was recommended by (Brown and Hafner, 2005), which takes into account the degrees of freedom in the PMF model and the additional constraints in place for each model run. This theoretical *Q* calculation Q_{th} is given as:

Q_{th} *= (# samples **x** # good species)+[(# samples **x** # weak species)/3] - (# samples **x** factors estimated)* **(A2.6)**

Both approaches have been taken into account for this study and it is likely that the actual value lies somewhere between the two.

In PMF, it is assumed that only the x_{ij}'s are known and that the goal is to estimate the contributions (g_{ik}) and the factors (or profiles) (f_{kj}). It is assumed that the contributions and mass fractions are all non-negative, hence the "constrained" part of the least-squares. Additionally, EPAPMF allows the user to say how much uncertainty there is in each x_{ij}. Species-days with lots of uncertainty are not allowed to influence the estimation of the contributions and profiles as much as those with small uncertainty, hence the "weighted" part of the least squares and the advantage of this approach over PCA.

Diagnostic outputs from the PMF models were used to guide the appropriateness of the number of factors generated and how well the receptor modelling was accounting for the input data. Where necessary, initial solutions have been 'rotated' to provide a better separation of factors (sources) that were considered physically reasonable (Paatero et al., 2002). Each PMF model run reported in this study is accompanied by the modelling statistics along with comments where appropriate.

A2.4 DATASET QUALITY ASSURANCE

Quality assurance of sample elemental datasets is vital so that any dubious samples, measurements and outliers are removed as these will invariably affect the results of receptor modelling. In general, the larger the dataset used for receptor modelling, the more robust the analysis. The following sections describe the methodology used to check data integrity and provide a quality assurance process that ensured that the data being used in subsequent factor analysis was as robust as possible.

A2.4.1 Mass reconstruction and mass closure

Once the sample analysis for the range of analytes has been carried out, it is important to check that total measured mass does not exceed gravimetric mass (Cohen, 1999). Ideally, when elemental analysis and organic compound analysis has been undertaken on the same sample one can reconstruct the mass using the following general equation for ambient samples as a first approximation (Cahill et al., 1989, Cohen, 1999, Malm et al., 1994):

Reconstructed mass = [Soil] + [OC] + [BC] + [Smoke] + [Sulphate] + [Seasalt] **(A2.7)**

where:

[Soil] = 2.20[Al] + 2.49[Si] + 1.63[Ca] + 2.42[Fe] + 1.94[Ti]

(note for the current study Fe was used to calculate Al. Si and Ca equivalent mass)

[OC] = Σ[Concentrations of organic compounds]

[BC] = Concentration of black carbon (soot)

[Smoke] = [K] − 0.6[Fe]

[Seasalt] = 2.54[Na]

[Sulphate] = 4.125[S]

The reconstructed mass (RCM) is based on the fact that the six composite variables or ‘pseudo’ sources given in equation A1.11 are generally the major contributors to fine and coarse particle mass and are based on geochemical principles and constraints. The [Soil] factor contains elements predominantly found crustal matter (Al, Si, Ca, Fe, Ti) and includes a multiplier to correct for oxygen content and an additional multiplier of 1.16 to correct for the fact that three major oxide contributors (MgO, K_2O, Na_2O) carbonate and bound water are excluded from the equation.

[BC] is the concentration of black carbon, measured in this case by light reflectance/absorbance. [Smoke] represents K not included as part of crustal matter and tends to be an indicator of biomass burning.

[Seasalt] represents the marine aerosol contribution and assumes that the NaCl weight is 2.54 times the Na concentration. Na is used as it is well known that Cl can be volatilised from aerosol or from filters in the presence of acidic aerosol, particularly in the fine fraction via the following reactions (Lee et al., 1999):

$$NaCl(p) + HNO_3(ag) \rightarrow NaNO_3(p) + HCL(g) \quad \textbf{(A2.8)}$$

$$2NaCl(p) + H_2SO_4(ag) \rightarrow Na_2SO_4(p) + 2HCL(g) \quad \textbf{(A2.9)}$$

Alternatively, where Cl loss is likely to be minimal, such as in the coarse fraction or for both size fractions near coastal locations and relatively clean air in the absence of acid aerosol, then the reciprocal calculation of [Seasalt] = 1.65[Cl] can be substituted, particularly where Na concentrations are uncertain. This calculation was used for the Water Street since Na concentrations were unavailable due to the glass fibre matrix.

Most fine sulphate particles are the result of oxidation of SO_2 gas to sulphate particles in the atmosphere (Malm et al., 1994). It is assumed that sulphate is present in fully neutralised form as ammonium sulphate. [Sulphate] therefore represents the ammonium sulphate contribution to aerosol mass with the multiplicative factor of 4.125[S] to account for ammonium ion and oxygen mass (i.e., $(NH_4)_2SO_4$ = ((14 + 4)2 + 32 + (16x4)/32)).

Additionally, the sulphate component not associated with seasalt can be calculated from equation A2.10) (Cohen 1999):

$$\text{Non-seasalt sulphate (NSS-Sulphate)} = 4.125\ ([S_{tot}] - 0.0543[Cl]) \quad \textbf{(A2.10)}$$

Where the sulphur concentrations contributed by seasalt are inferred from the chlorine concentrations, i.e., [S/Cl]seasalt = 0.0543 and the factor of 4.125 assumes that the sulphate has been fully neutralised and is generally present as $(NH_4)_2SO_4$ (Cahill, Eldred *et al*. 1990; Malm, Sisler *et al*. 1994; Cohen 1999).

The RCM and mass closure calculations using the pseudo-source and pseudo-element approach are a useful way to examine initial relationships in the data and how the measured mass of species in samples compares to gravimetric mass. Note that some scatter is possible because not all aerosols are necessarily measured and accounted for, such as all OC, ammonium species, nitrates and unbound water.

As a quality assurance mechanism, those samples for which RCM exceeded gravimetric mass or where gravimetric mass was significantly higher than RCM were examined closely to assess gravimetric mass and IBA data. Where there was significant doubt either way, those samples were excluded from the receptor modeling analysis. The reconstructed mass calculations and pseudo source estimations are presented in the appendices at the end of this report.

A2.4.2 Dataset preparation

Careful preparation of a dataset is required because serious errors in data analysis and receptor modeling results can be caused by erroneous individual data values. The general methodology followed for dataset preparation was as recommended by (Brown and Hafner, 2005). For this study, all data were checked for consistency with the following parameters:

1. Individual sample collection validation;
2. Gravimetric mass validation;
3. Analysis of RCM versus gravimetric mass to ensure RCM < gravimetric;
4. Identification of unusual values including noticeably extreme values and values that normally track with other species (e.g., Al and Si) but deviate in one or two samples. Scatter plots and time series plots were used to identify unusual values. One-off events such as fireworks displays, forest fires or vegetative burn-offs may affect a receptor model as it is forced to find a profile that matches only that day;

5. Species were included in a dataset if at least 70% of data was above the LOD and signal-to-noise ratios were checked to ensure data had sufficient variability. Important tracers of a source where less than 70% of data was above the LOD were included but model runs with and without the data were used to assess the effect;
6. For PCA, % errors and signal-to-noise ratios were used as a guide as to whether a species was too 'noisy' to include in an analysis.

In practice during data analyses, the above steps were a reiterative process of cross checking as issues were identified and corrected for, or certain data excluded and the effects of this were then studied.

A2.4.2.1 PMF data matrix population

The following steps were followed to produce a final dataset for use in the PMF receptor model (Brown and Hafner, 2005).

Below detection limit data: For given values, the reported concentration used and the corresponding uncertainty checked to ensure it had a high value.

Missing data: Substituted with the dataset median value for that species.

A2.4.2.2 PMF uncertainty matrix population

Uncertainties can have a large effect on model results so that they must be carefully compiled. The effect of underestimating uncertainties can be severe, while overestimating uncertainties does not do too much harm (Paatero and Hopke, 2003).

Uncertainties for data: Data was multiplied by % fit error provided by IBA analysis to produce an uncertainty in ng m^{-3}.

Below detection limit data: Below detection limit data was generally provided with a high % fit error and this was used to produce an uncertainty in ng m^{-3}. Zero data was given a corresponding uncertainty value of 5/6×LOD.

Missing data: Uncertainty was calculated as 4 × median value over the entire species dataset.

BC: Because of high mass values for BC, the uncertainties were generated by multiplying mass values by a factor of four to down-weight the variable.

PM gravimetric mass: Uncertainty given as 4 × mass value to down-weight the variable.

Reiterative model runs were used to examine the effect of including species with high uncertainties or low concentrations. In general it was found that the initial uncertainty estimations were sufficient and that adjusting the 'additional modelling uncertainty' function accommodated any issues with modelled variables such as those with residuals outside ± 3 standard deviations.

www.gns.cri.nz

Principal Location

1 Fairway Drive
Avalon
PO Box 30368
Lower Hutt
New Zealand
T +64-4-570 1444
F +64-4-570 4600

Other Locations

Dunedin Research Centre
764 Cumberland Street
Private Bag 1930
Dunedin
New Zealand
T +64-3-477 4050
F +64-3-477 5232

Wairakei Research Centre
114 Karetoto Road
Wairakei
Private Bag 2000, Taupo
New Zealand
T +64-7-374 8211
F +64-7-374 8199

National Isotope Centre
30 Gracefield Road
PO Box 31312
Lower Hutt
New Zealand
T +64-4-570 1444
F +64-4-570 4657